

# 2240

# **POTENTIAL SOLAR RADIATION AT THE H. J. ANDREWS EXPERIMENTAL FOREST**

Interim Report on research performed under U. S. D. A. Forest Service, Pacific Northwest Research  
Station, Cooperative Agreement N. PNW 93-0477

David Greenland  
Department of Geography  
University of Oregon  
Eugene, Oregon 97403-1251

January 31, 1996

## POTENTIAL INSOLATION MAPS OF THE H. J. ANDREWS EXPERIMENTAL FOREST.

### ABSTRACT

Solar radiation is ultimately the driver of virtually all ecological and atmospheric systems. This study uses a model to compute the potential clear-sky radiation receipt on the slopes of the H. J. Andrews Experimental Forest Long-Term Ecological Research site in the foothills of the southern Cascade mountains of central Oregon. A comprehensive review of available modeling methods for solar radiation in complex terrain is provided. The method developed by Williams is selected and applied to the forest area for the times of the solstices and equinox. It is also applied at month times in January, February, April, and May in order to completely characterize the seasonal change of potential radiation at the location. The method uses an 82 x 111 point grid with a 120 m spacing interval. Resulting maps reveal areas of the Forest with extremely steep gradients of potential radiation. These steep gradients have higher absolute values in summer compared to winter. The south-facing slopes which have the highest potential radiation values tend to be at the highest elevations. There are places which receive no direct radiation as far into the year as February. Standard deviation values of potential radiation across the Andrews show the maximum spatial variability to occur in February. There is a decrease in the ratio of diffuse to direct plus diffuse potential radiation from 0.66 at Dec. 21 to 0.23 at June 21. It seems that Lookout Creek approximately divides the Andrews Forest into an area of relatively high potential radiation to the north of the Creek and relatively lower potential radiation values to the south of the Creek. The results are also discussed in relation to spatial distributions of the values of other biophysical variables available on the Andrews Geographic Information System. Potential radiation values seem to be associated with the spatial distributions shown on the data layers of debris flows and predominant tree species zones. A comprehensive series of appendices documents the procedures used so they that they can be employed to other parts of the forests of the Pacific Northwest and in other areas of complex terrain. Digital versions of the input data, program codes, output results, and other relevant material are also provided.

## TABLE OF CONTENTS

Abstract	...	1
Table of Contents	...	2
List of Figures	...	3
Symbols	...	4
Introduction	...	6
The Climate of the H. J. Andrews Experimental Forest	...	7
Modeling Solar Radiation	...	8
Direct Radiation	...	8
Diffuse and Terrain-Reflected Radiation	...	9
Commonly Used Radiation Models	...	9
Radiation Models Employed at the Andrews Forest	...	14
Discussion	...	16
The Williams Model	...	16
Procedure	...	17
Overview	...	17
Preliminary Steps	...	18
Data Preparation	...	18
Observed Radiation Data at the Andrews	...	19
Estimation of Atmospheric Transmissivity	...	19
Application of ANRAD	...	20
The Potential Radiation Maps	...	20
Individual Maps	...	21
Time Series of Maps	...	22
Comparison of Potential Radiation Maps to Other GIS		
Data Layer Spatial Distributions	...	23
Application of Methodology to Other Areas	...	24
Discussion and Conclusions	...	24
Future Work	...	25
Acknowledgments	...	26
References	...	26
Glossary	...	31
Appendices	...	32
Appendix 1 Universal Transverse Mercator (UTM) Coordinates	...	32
Appendix 2 The SKIP Program	...	32
Appendix 3 The ELDAT Program	...	32
Appendix 4 The ANRAD Program and SURFER	...	33
Appendix 5 Data used for estimation of Extraterrestrial Radiation	...	36

## LIST OF FIGURES

- Fig 1. Location of the H. J. Andrews Experimental Forest
- Fig 2. Topographic surface map of the H. J. Andrews Experimental Forest
- Fig 3. Geometry of radiation arriving at a sloping surface (After Sellers, 1965, Duguay, 1993)
- Fig 4. Daily totals of shortwave radiation at the Primary Meteorological Station, 1994.
- Fig 5. Daily totals of shortwave radiation at Vanilla Leaf Station, 1994.
- Fig 6. Potential direct and diffuse radiation over the H. J. Andrews Experimental Forest for June 21 presented without the infilling of isolines.
- Fig 7. Potential direct and diffuse radiation over the H. J. Andrews Experimental Forest for Dec 21.
- Fig 8. Potential direct and diffuse radiation over the H. J. Andrews Experimental Forest for Jan 15.
- Fig 9. Potential direct and diffuse radiation over the H. J. Andrews Experimental Forest for Feb 15.
- Fig 10. Potential direct and diffuse radiation over the H. J. Andrews Experimental Forest for Mar 21.
- Fig 11. Potential direct and diffuse radiation over the H. J. Andrews Experimental Forest for April 15.
- Fig 12. Potential direct and diffuse radiation over the H. J. Andrews Experimental Forest for May 15.
- Fig 13. Potential direct and diffuse radiation over the H. J. Andrews Experimental Forest for June 21.

Back Folder      Transparency copy of Fig. 2 for overlaying on Figs. 7 - 13.

## SYMBOLS

### *Arabic Letters*

#### Lower case

d	actual distance between the Earth and the sun at a given time, orbital vector or radius (often also symbolized as r).
$d_m$	mean distance between the Earth and the sun
h	hour angle
i	angle of incidence of direct radiation between the normal to the slope and the solar beam at a given time
$i_h$	angle of incidence of the solar beam referenced to a horizontal surface
$i_0$	incident angle of $S_x$ at TOA (see Dubayah, 1990)
$k_a$	an approximation of atmospheric absorption
$k_s$	an approximation for atmospheric scattering
$k'$	anisotropy index (Hay, 1983)
ly	langley ( $1 \text{ cal cm}^{-2} \text{ min}^{-1}$ )
m	optical depth
p	mean zenith angle path transmissivity
s	slope of the surface (slope angle)

#### Upper case

$A_z$	solar azimuth - direction from observation point to the sun
$A_z'$	relative azimuth - the absolute difference between the aspect of the surface and the solar azimuth
$A_s$	slope azimuth (aspect)
D	Diffuse radiation
$D_h$	diffuse radiation on a horizontal surface
$D_{tr}$	terrain reflected shortwave radiation
DRAD	daily potential solar radiation for the slope-aspect combination (see Duan et al. 1994)
F	$1 - (D_h / K_h)^2$ (see Klucher, 1979)
$F\downarrow$	downward flux of radiation through the atmosphere (see Dubayah et al, 1990)
$H_s$	sunrise/sunset hour angle (see Bonan, 1989)
$I_o$	Solar constant
$I_{o60}$	solar constant for a 60 minute period (see Swift, 1976).
J	Julian day number
$K\downarrow$	global solar radiation
$K_h$	(D+S) on a horizontal surface. Same as $K\downarrow$ but refers only, and specifically, to a horizontal surface
$K_t$	Fraction of $K_h$ that is diffuse radiation (see Bonan, 1989)
L	latitude
$L_1$	latitude of an equivalent slope (see Swift, 1976)
$L_2$	time offset in hour angle between the actual and the equivalent slopes (see Swift, 1976)
NDVI	Normalized Difference Vegetation Index
PR	potential radiation
$Q^*$	net radiation
$R_f$	conversion factor for converting $S_h$ to S on a slope
RAJ	ratio of measured horizontal surface radiation, $K_h$ , to potential clear sky radiation
RDC	intercept of the sky cover-daily air temperature range for month MO
RDM	slope of the sky-cover daily air temperature range for month MO
S	Direct radiation

$S_h$	direct solar radiation to an unobstructed horizontal surface
$S_n$	direct radiation on a plane normal to the sun
$S_x$	incoming shortwave radiation at the top of the atmosphere (TOA), extra terrestrial radiation
SKY	sky cover value
$T_2$	hour angle of sunrise on the slope
$T_3$	hour angle of sunset on the slope
TMX and TMN	are observed maximum and minimum daily air temperatures
TOA	Top of the atmosphere
$V_f$	A sky view factor (see Nunez, 1980)
$V_s$	direct radiation shading factor (see Dozier, 1980)
$Z_s$	zenith angle

*Greek Letters*

$\alpha$	albedo
$\alpha_D$	albedo for diffuse radiation
$\alpha_S$	albedo for direct radiation
$\delta$	solar declination angle
$\kappa$	ratio of diffuse sky irradiance to global insolation at the Earth's surface
$\mu m$	micrometer, 1 millionth of a meter.
$\tau_K$	clearness index

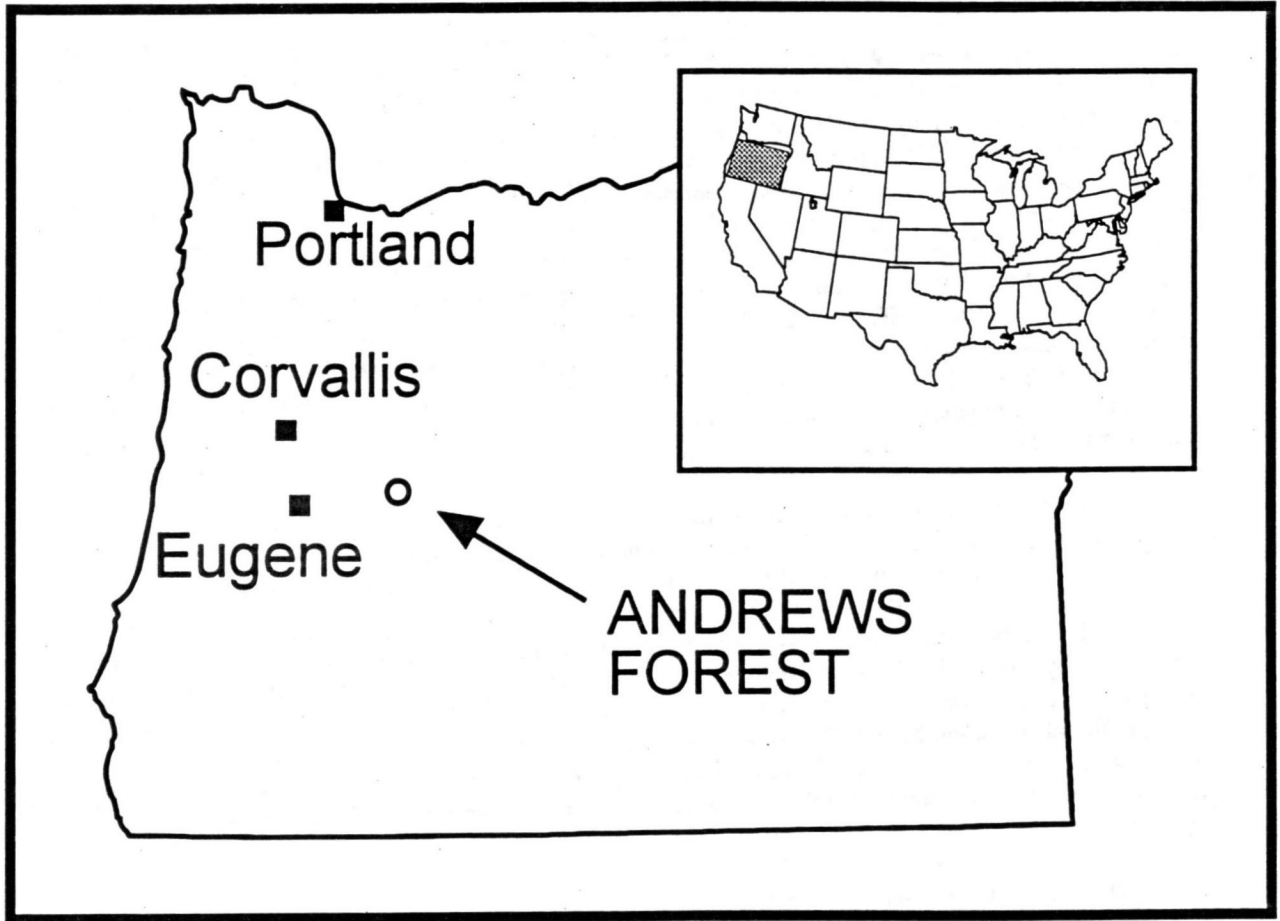


Fig 1. Location of the H. J. Andrews Experimental Forest

# POTENTIAL INSOLATION MAPS OF THE H. J. ANDREWS EXPERIMENTAL FOREST

## INTRODUCTION

Solar radiation, also called insolation, is ultimately the driver of virtually all ecological, and atmospheric systems. It specifically provides the energy source for photosynthetic activity and the hydrologic cycle. Under cloud-free conditions there is a large spatial and temporal variation of the actual amount of radiation arriving at different slopes at different times of the year in an area of complex topography such as the H. J. Andrews Experimental Forest in Oregon. This study seeks to examine this spatial and temporal variation.

The H. J. Andrews Experimental Forest (HJA) is a 6400 ha forest of Douglas Fir (*Pseudotsuga menziesii* (Mirb.) Franco), Western Hemlock (*Tsuga heterophylla* (Raf.) Sarg.), and Pacific Silver Fir (*Abies amabilis* Doug. ex Forbes) located in, and typical of, the central portion of the western slope of the Cascade mountain range of Oregon (Fig. 1). The forest is currently one of 18 sites in the Long-Term Ecological Research (LTER) program sponsored by the National Science Foundation (Franklin et al., 1990). During the 1970s the Forest was a representative site in the Coniferous Forest Biome Project of the U.S. International Biological Program. It was originally established in 1948 as an Experimental Forest of the U.S. Forest Service. There is an immense legacy of research resulting from the participation of the Andrews Forest in these research programs (McKee. et al., 1987, Blinn et al., 1988). Future participation in LTER ensures the continuing scientific importance of the site. Climatological information has been collected at the site since 1951 with a continuous, electronically sensed, record from May 1972. Until 1994, the observing system is composed of a primary meteorological station and a network of satellite temperature and precipitation recording stations. After 1994, four primary benchmark stations anchored the observing system.

The purpose of this study is to produce maps of seasonal potential insolation (i.e. solar radiation receipt under clear sky conditions) for the H. J. Andrews Experimental Forest. These maps will have value: a) in making future estimates of heat energy input to the various slopes of the forest, b) establishing relationships between solar input and net primary productivity, and c) identifying areas of greatest potential heat input - a process which has implication for driving mesoscale wind circulations in the area, and possibly also for establishing areas of potential forest fire initiation danger. The research is performed in such a way as to make the results compatible with the Andrews LTER GIS data base as well as with Digital Elevation Model (DEM) data of other areas of the Pacific Northwest already existing at the Forest Sciences Laboratory (FSL) at Corvallis. The research is also consistent with a larger planned study designed for estimating possible climate change resulting from different forest management practices.

The specific objectives in this study are to :

1. Review algorithms for estimating potential insolation (i.e. solar radiation receipt under clear sky conditions).
2. Select the most efficient available algorithm for microcomputing systems for application to the H. J. Andrews Forest and apply the algorithm for the periods of the summer and winter solstices and the equinoctial periods and selected intervening periods.
3. Adapt the selected algorithm for use with the Forest Sciences Laboratory (FSL) LTER-GIS system and establish compatibility with ERDAS GIS and Digital Elevation Model data for the PNW already existing at the FSL.

The following products of the research are:

1. Hard copies of seasonal maps of potential insolation for the H. J. Andrews Forest provided in this research report.
2. Digital data layers representing the output from the first product and which can be added to the Andrews LTER GIS. These data are provided, along with other relevant information, on the diskette at the end of this report.
3. A description of the research which is provided by this report and which includes a series of appendices outlining how the procedures may be applied to elevation data from other parts of the PNW or any other area.

I will first describe the climate of the H. J. Andrews Experimental Forest. Then, given the objectives outlined above, the report falls into three sections. First, there is a review of algorithms and methodologies employed for making potential insolation estimates in complex terrain. This review includes a description of the methods already applied to the Andrews Forest for purposes of driving functional ecological and distributed hydrological models. Second, there is a description of the procedure employed to produce the potential radiation maps in this report. This includes a discussion of the maps, their major features, possible relations to the spatial distribution of other biophysical phenomena at the Andrews Forest, and how the results and procedures from this research may be used in future studies on the effect of forest management practices on the albedo (reflectivity) and subsequent physical climatology of the Forest. Finally, there is a substantive series of appendices which collectively provide details of how the estimates were made, digital copies of the required computer programs, and a discussion of the necessary steps for applying the procedure to other areas.

### **The Climate of H. J. Andrews Experimental Forest**

The primary meteorological station of HJA is at an elevation of 426 m (1397 ft) at latitude 44° 15' N and longitude 122° 10' W (Fig. 2). HJA occupies the Lookout Creek watershed which ranges from 420 to 1630 m (1378 to 5346 ft) and drains into the Blue River. Below 1050 m (3444 ft), the Western Hemlock zone is found and is characterized by Western Hemlock and Douglas Fir. Above 1050 m (3444 ft) the Pacific Silver Fir zone is established (Bierlmaier and McKee, 1989). The large height of these dominant species can play a significant role in shading the ground surface from direct radiation. Western Hemlock, Douglas Fir, and Pacific Silver Fir may grow to heights of 61 m (200 ft), 76 m (250 ft), and 55 m (180 ft) respectively (Jensen and Ross, 1994).

Bierlmaier and McKee (1989) have described the HJA climate as being wet and fairly mild in winter and warm and dry in summer. They emphasize the role of the polar front jet stream in funneling into the area one low pressure zone and frontal storm after another during the winter. Precipitation comes mainly from cold or occluded fronts. The storms are slowed by the Coast and Cascade ranges and are consequently of long duration and low intensity. The summer season is dominated by the establishment of a ridge of high pressure along the coast and the eastern Pacific. Consequently this season is characterized by highly stable air and low precipitation amounts. During the period 1973 to 1984 the average annual temperature was 8.5° C (47.3° F). Monthly temperatures ranged from 0.6° C (33.1° F) in January to 17.8° C (64.0° F) in July. The annual average precipitation was 2302 mm (90.6 ins) 71% of which fell from November through March. At 1203 m (3946 ft) annual precipitation rises to 2785 mm (109.7 ins). Above 1050 m (3444 ft) a persistent snowpack up to 4 m (13 ft) deep may form and last into June (Bierlmaier and McKee, 1989). Further details of the climatography and climatology of HJA may be found in Emmingham and Lundburg (1977 - quoted by (Bierlmaier and McKee, 1989)), Waring et al. (1978), McKee and Bierlmaier (1987) and Greenland (1994).

# ANDREWS FOREST TOPOGRAPHY

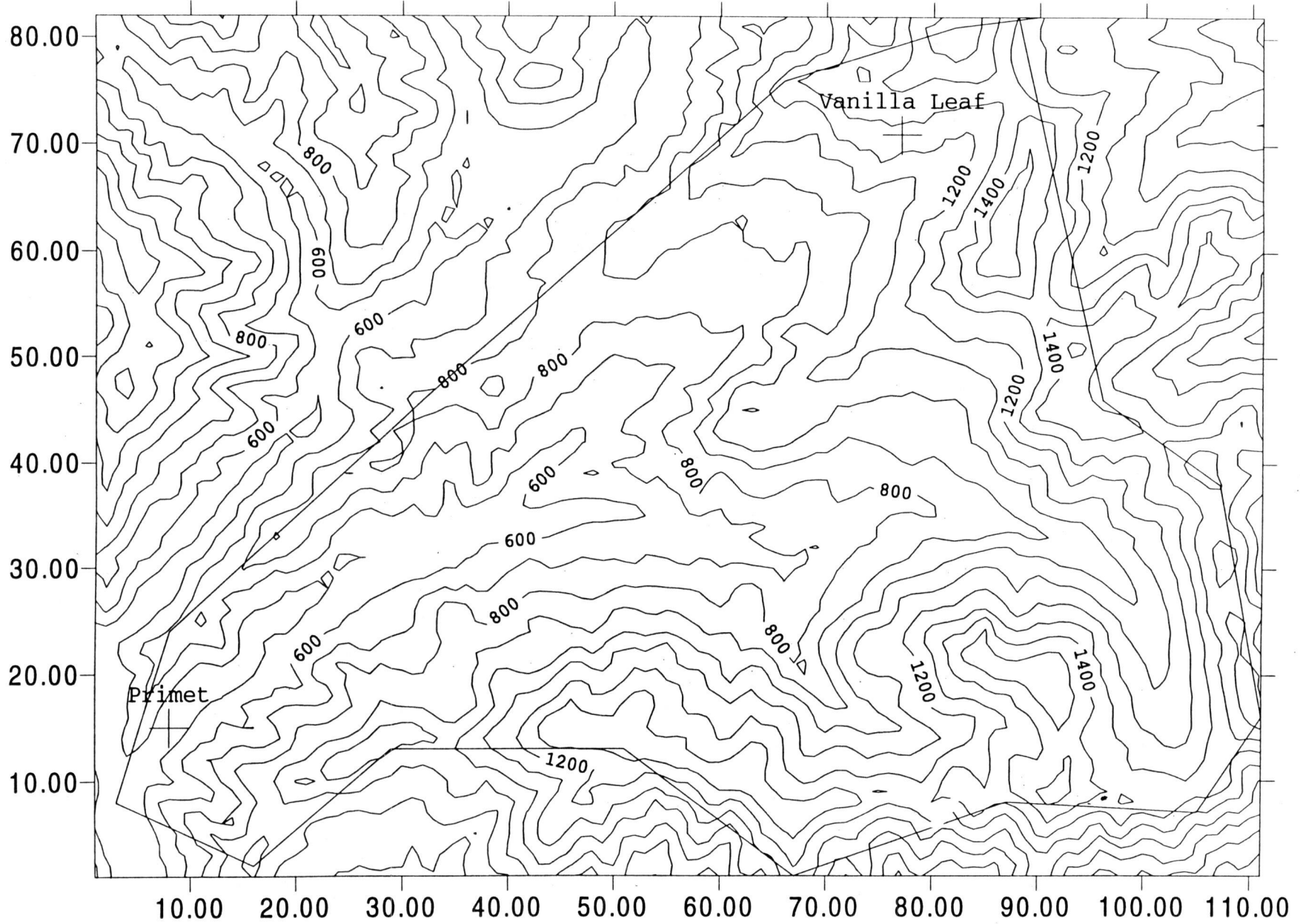


Fig. 2. Topographic surface map of the H. J. Andrews Experimental Forest

Axis units are 120 m (e.g 10 = 120x120 m from lower left hand corner of the map)  
North is to the top of the map. Countours are in m above msl. Straight lines  
indicate the approximate boundary of the Andrews Forest.

The complex terrain indicated in Fig. 2 gives rise to a wide variety of values of potential radiation arriving at the different slopes of the area. Since it is impracticable to measure radiation on all these slopes it is necessary to employ modeling approaches. The problem of modeling radiation receipt in complex terrain has received much attention. In the next section I review some of the more common methods which have been developed.

## MODELING SOLAR RADIATION

The modeling of solar radiation receipt, insolation, at a particular location on the Earth's surface began in the 1960s. Previous to that global and latitudinal estimates had been commonly found in atmospheric science texts and reports (Budyko, 1956, London, 1957). Modeling for a specific location, and particularly for slopes in complex terrain, has been driven by the needs of a variety of Earth Science disciplines such as hydrology, climatology, ecology, forestry, geomorphology, and glaciology as well as by the needs of solar engineering and architects along with the parallel interests of some physicists and investigators from the remote sensing community. An excellent review of the modeling of radiation and net radiation in complex terrain has been provided by Duguay (1993). A useful review of modeling and observation of radiation and energy budgets of mountain environments has also been given by Saunders and Bailey (1994) who concentrate on alpine tundra surfaces. Here, I will use the part of Duguay's review dealing with shortwave irradiance as a basis for an introduction to the subject. The review presented here goes much further than that of Duguay but even so is not exhaustive. Readers who pursue the references listed in this review will find many other studies beside those treated here. I have selected those studies which provide most relevance to investigations at the Andrews forest. I will also use the same symbols employed by Duguay. Many different symbols and terms are used for the large number of variables found in radiation studies. A list of symbols and a glossary of meanings is provided in this report in order to provide as much precision and clarity as possible.

Solar radiation, also called global solar radiation or solar irradiance, is the radiation arriving at the Earth from the sun. It is also called shortwave radiation and is in the wavelength band 0.15 to 3.00  $\mu\text{m}$  (Oke, 1987). Different authors quote somewhat different wavelengths including 0.28 to 5.00  $\mu\text{m}$  (Duguay, 1993) and 0.20 to 4.00  $\mu\text{m}$  (Hartmann, 1994). The differences in these ranges are effectively minor since by far the greatest amount of shortwave radiation arrives towards the middle of the range and only a very small quantity arrives at the limits of the range. In the absence of clouds, solar radiation arrives at the Earth's surface in two classes. Direct radiation (S) is that part of the solar beam which arrives at the surface without any interaction at all with the Earth's atmosphere. Diffuse radiation (D) is shortwave radiation scattered downwards to the Earth's surface after striking molecules of the component atmospheric gases and aerosols together with shortwave radiation subsequently scattered back to the Earth after being reflected upwards by the Earth's surface and atmospheric components.

### Direct Radiation

The amount of direct radiation arriving at a horizontal surface when there is no absorption in the atmosphere is given by:

$$S = I_0(d_m / d)^2 \cos Z_s \quad \text{--- 1}$$

where  $I_0$  is the solar constant,  $d_m$  is the mean distance between the Earth and the sun,  $d$  is the actual distance between the Earth and the sun at the time of estimation, and  $Z_s$  is the zenith angle. Equation 1 may be used to estimate the amount of radiation arriving at the outside of the atmosphere since

$$\cos Z_s = \sin L \sin \delta + \cos L \cos \delta \cos h \quad \text{--- 2}$$

where  $L$  is latitude,  $\delta$  is solar declination, and  $h$  is the hour angle. Hartmann (1994) has provided a useful equation for computing the daily total radiation arriving at the top of the atmosphere (TOA). It is

$$S_{\text{day}} = (I_0/\pi)(d_m / d)^2 (T_2 \sin L \sin \delta + \cos L \cos \delta \sin T_2) \quad \text{--- 3}$$

where  $T_2$  is the hour angle of sunrise (or sunset) and must be entered in radians. Assuming  $(d_m / d)$ , sometimes called the orbital vector, to be unity, the amount of radiation arriving on a sloping surface under these conditions is given by relating slope and solar geometries through the angle of incidence,  $i$ , the angle of incidence of direct radiation between the normal to the slope and the solar beam at a given time, as follows:

$$S = S_h (\cos i / \cos i_h) \quad \text{--- 4}$$

where  $i_h$  is the angle of incidence of the solar beam referenced to a horizontal surface. The angle of incidence,  $i$ , is given by:

$$i = \cos^{-1} \{ \cos(s) \cos(Z_s) + \sin(s) \sin(Z_s) \cos(A_z + A_s) \} \quad \text{--- 5}$$

where  $s$  is the slope of the surface,  $A_z$  is the solar azimuth, and  $A_s$  is the slope azimuth (aspect). These relationships and angles are demonstrated in Fig. 3. Daily totals of potential shortwave radiation received on a slope may be obtained by integrating, over daylight hours, values from equation 1.

### Diffuse and Terrain-Reflected Radiation

The value of diffuse radiation depends upon  $Z_s$  through its relation with the optical depth ( $m$ ), the turbidity of the atmosphere, the wavelength of the light, and the amount of sky visible at the observation point i.e. the sky view factor. Diffuse radiation is often assumed to be equally distributed from all parts of the sky (isotropic) but, in reality, its intensity is greatest nearest the sun. Unequal sky distribution of  $D$  is called an anisotropic distribution. The sum of direct and diffuse solar radiation is sometimes called global solar radiation and is symbolized by  $K\downarrow$ . Tests of modeling schemes for  $D$  sometimes make use of variables called the clearness index,  $\tau_K$ , and  $\kappa$ , the ratio of diffuse sky irradiance to global insolation at the Earth's surface.  $\tau_K$  is  $K_h / S_x$ , where  $S_x$  is the solar radiation at the top of the atmosphere (TOA).

Shortwave radiation reflected to a point from surrounding terrain surfaces may be important when the cosine of  $i$  approaches zero especially when the surrounding surfaces are highly reflective as in snow covered conditions. Many modeling exercises neglect terrain reflected radiation, ( $D_{tr}$ ).

### Commonly Used Radiation Models

Richard Lee (1963) may have been the first person to address the problem of estimating radiation values on local slopes. He produced extensive tables of his results for different slopes, latitudes, and times of the year. Similar tables were produced by Buffo et al. (1972). After the pioneering effort of Lee there followed a series of important papers on the topic as described below.

#### *Garnier and Ohmura (1968)*

The initial classic study of radiation modeling on slopes was performed by Garnier and Ohmura (1968). They suggested estimating  $K\downarrow$  by

$$K\downarrow = S_x p^m \cos(i) + D_h \cos^2(s/2) + \alpha (S_h + D_h) \sin^2(s/2) \quad \text{--- 6}$$

where  $S_x$  is incoming shortwave radiation at the top of the atmosphere, i.e. extraterrestrial radiation,  $p$  is the mean zenith angle path transmissivity,  $D_h$  is the diffuse radiation on a horizontal surface,  $\alpha$  is the albedo of the surface, and  $S_h$  is the direct radiation on a horizontal surface. The first and second terms

represent S and D respectively and the third term represents  $D_{tr}$ . Garnier and Ohmura suggested using actual site measurements to determine the value of p at the site and that p should be approximated by  $\sec Z_s$ . The second and third terms assume an isotropic distribution of D. The third term was not used in practice.

*Ferguson et al. (1971)*

The first local radiation maps of a whole watershed of which I am aware were produced for the Marmot Creek experimental watershed area in Alberta by Ferguson et al. (1971). Ferguson's group used approaches similar to that in equation 1 and employed specific transmission values for atmospheric components. It is remarkable that the calculations for the maps were performed by hand.

*Williams et al. (1972)*

Williams et al. (1972) provided estimates of  $K\downarrow$  for complex terrain which treated the terrain as a matrix of elevation points and allowed for the shading of an individual point, where appropriate, by those points surrounding it. Their estimate of D is given by

$$D = (I_0 / d^2) (0.91 - p^m) \cos(Z_s) \cos^2(s/2) \quad \text{--- 7}$$

0.91 represents the proportion of radiation which has not been absorbed by atmospheric constituents. This model corrects the value of m for the elevation of the observation point.

*Swift (1976)*

The approach of Swift (1976) for modeling potential solar radiation on slopes has found most circulation in the field of hydrology. It has been an attractive approach because it requires only Julian dates, slope angle and azimuth and latitude in its application. Swift bases his method on an integrated equation derived by Okanoue (1957, quoted by Swift, 1976) and used in Lee's original study (Lee, 1963). The core of the model estimates the potential solar radiation on a slope as

$$S = I_{060} \{(\sin \delta \sin L_1)(T_3 - T_2)/15 + \cos \delta \cos L_1 [\sin(T_3 + L_2) - \sin(T_2 + L_2)]/12/\pi\} \quad \text{--- 8}$$

where  $I_{060}$  is the solar constant for a 60 minute period,  $\delta$  is the solar declination angle,  $L_1$  is the latitude of an equivalent slope,  $T_3$  is the hour angle of sunset on the slope,  $T_2$  is the hour angle of sunrise on the slope, and  $L_2$  is the time offset in hour angle between the actual and the equivalent slopes. Swift and Knoerr (1973) showed that a slope factor  $S/S_h$  could be used to estimate the actual solar radiation. Actual transmission factors are taken into this scheme by the use of actual observations of  $K\downarrow_h$ . There is no resolution between S and D in this methodology. The way the application of the slope factor is explained it seems to imply that  $K\downarrow_h$  is assumed to be equivalent to  $S_z$ . D is not mentioned at all. The method was not tested against observed data in the original paper.

*Dozier and Outcalt (1979)*

The paper of Dozier and Outcalt (1979) was one of the first attempts to allow for  $D_{tr}$ . Direct radiation was estimated as

$$S = (I_0 / d^2) \cos(i) \exp(k_a + k_s) \quad \text{--- 9}$$

where  $k_a$  is an approximation of atmospheric absorption and  $k_s$  is an approximation for atmospheric scattering. The term for estimating diffuse radiation was formulated to allow for  $D_{tr}$  as

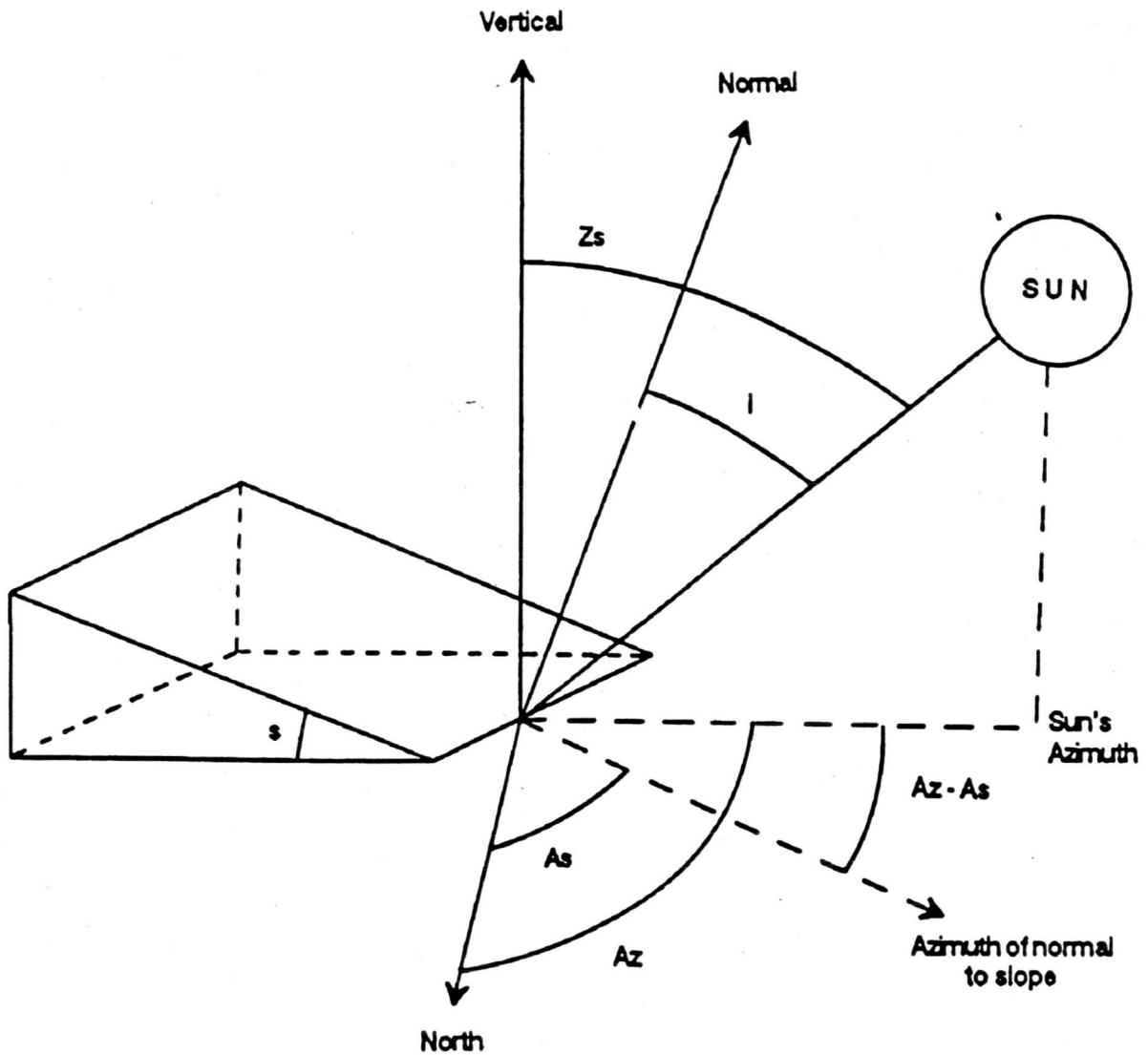


Fig 3. Geometry of radiation arriving at a sloping surface (After Sellers, 1965, Duguay, 1993)

$$D = 0.5\{1 - \exp(k_s)\} (S_h / d^2) \{\cos^2(s/2) + 0.5 \alpha_D(1 - \exp(k_s)) + \alpha_S S_h\} \quad \text{--- 10}$$

where  $\alpha_D$  is the albedo for diffuse radiation and  $\alpha_S$  is the albedo for direct radiation. When  $Z_s > 50^\circ$   $\alpha_S$  is not equal to  $\alpha_D$  and must be corrected for glint effects.

*Klucher (1979)*

Klucher (1979) modified a model by Temps and Coulson (1977) by using a function which reduced the model to the isotropic approximation under overcast conditions. The Klucher model is written

$$K\downarrow = S_n \cos i + D_h (1 + \cos s) \{(1 + F \sin^3(s/2)) (1 + F \cos^2 i \sin^3 i')\} + 0.5 \alpha K_h (1 - \cos s) \{0.5 (1 - \cos i')\} (|\cos A_z'|) \quad \text{--- 11}$$

where  $F$  is  $1 - (D_h / K_h)^2$  and  $A_z'$  is the relative azimuth - the absolute difference between the aspect of the surface and the solar azimuth. The model incorporates an increase in diffuse radiation near the horizon. This feature was found to decrease the accuracy of models when tested at high elevation (Isard, 1986)

*Nunez (1980)*

Nunez (1980) used standard meteorological data to obtain  $S$  and  $D$  with a model based on equation 1 and allowing for variable transmission factors for atmospheric components.  $D$  was calculated from

$$D = D_h V_f + (1 - V_f) K_h \alpha \quad \text{--- 12}$$

where  $V_f$  is a sky view factor and  $K_h$  is  $(D+S)$  on a horizontal surface. Only the horizon angle is taken into account in the calculation of  $V_f$  as opposed to also using slope and aspect effects.

*Dozier (1980)*

The first person to consider specification of the wavelength bands in radiation modeling schemes for the surface was Dozier (1980) who was interested in applying the schemes to remotely sensed data. Transmissivities and Rayleigh scattering are atmospheric component and wavelength specific in this model. Dozier estimates  $S$  for a slope by

$$S = S_n \cos i (1 - V_s) \quad \text{--- 13}$$

where  $S_n$  is the radiation on a plane normal to the sun and  $V_s$  is a direct radiation shading factor which is time consuming to estimate. Dozier introduces shading factors both for local forest ( $V_s$ ) and for surrounding terrain. He also is the first to attempt to treat anisotropic diffuse radiation.  $D_{tr}$  is computed as the sum of reflected diffuse radiation and diffuse reflectance of direct radiation from adjacent terrain. Dozier (pers. comm. 1982) devised a faster terrain searching algorithm than was employed by Williams et al (1972).

*Brühl and Zhunkowski (1983)*

Brühl and Zhunkowski (1983) use a multilayer atmospheric transfer model to compute S and D at the boundary layer. Sounding data and the volume of atmospheric aerosols are needed. The method also takes into account multiple reflections between mountain slopes. It has not been used very much due to it being computationally intensive.

*Hay (1983)*

Hay (1983) developed an "anisotropy index" for use with Kondratyev and Manolova's (1960) earlier model. The resulting model becomes

$$K_{\downarrow} = S_n \cos i + D_h \{k' (\cos i / \cos i_h) + 0.5 (1-k') (1 + \cos s) + 0.5 \alpha K_h (1 - \cos s)\} \quad \text{--- 14}$$

where  $k'$  is the anisotropy index which is given by  $S_n / S_n^T$  where  $S_n^T$  is the solar flux density to a surface oriented normal to the sun at the TOA. The index is found by integrating transmission values of S.

*Isard (1986)*

Isard tested a number of models which estimated radiation on slopes at the high elevation Niwot Ridge, Colorado site. He found that models based on the correlation between the clearness index and  $\kappa$  fitted observed data almost as well as those using measurements of normal direct beam irradiation ( $S_n$ ). Errors in prediction methods which use measurements of  $S_n$  to resolve S and D are small for completely clear and overcast times but are larger for partly cloudy conditions. Accuracy of estimations of  $K_{\downarrow}$  decrease with an increase of slope angle. Use of models incorporating the solar anisotropic assumption improves estimates for slopes facing directly into or away from the sun.

*Bonan (1989)*

Bonan (1989) used the methodology of Liu and Jordan (1960, 1962, 1963) and Klein (1977) which decomposes  $K_h$  into S and D and then uses tilt factors to adjust  $K_h$  to become  $K_{\downarrow}$  for the slope in question. Following Klein (1977) Bonan estimates  $S_x$  as

$$S_x = I_0 / \pi \{1 + 0.333 \cos (360 J / 365)\} * \{\cos L \cos \delta \sin H_s + (H_s \pi / 180) \sin L \sin \delta\} \quad \text{--- 15}$$

where J is the Julian day number, L is latitude,  $H_s$  is the sunrise/sunset hour angle. Bonan used linear regressions of monthly values of observed  $K_h$  and cloud data to estimate the attenuation of solar radiation passing through the atmosphere. He used separate regression equations for North America, Scandinavia, and the former Soviet Union. Data points in the regression were 10 or less. The fraction ( $K_t$ ) of  $K_h$  that is diffuse radiation is based on the fraction of the  $S_x$  transmitted through the atmosphere where

$$K_t = K_h / S_x \quad \text{--- 16}$$

and  $D / K_h$  is given as a function of  $K_t$  in a somewhat circular fashion. Bonan uses tilt factors to estimate radiation received on slopes. A tilt factor is defined as the ratio of radiation received on a tilted surface to that received on a horizontal surface (i.e.  $S/S_h$ ) (c.f. Swift and Knoerr, 1973) and is estimated using a series of equations formulated by Keith and Kreider (1978). An isotropic assumption is used for

D. The proportion of D arriving at a sloping surface is adjusted for the amount of sky observable from the slope. Tilt factors are used separately for S and D and S and D are combined to give  $K\downarrow$  for the slope.

The methodology was not tested rigorously. It was tested against data from one site in Alaska and against values of  $K_h$  for northern North America modeled earlier by Hare and Hay (1974).

*Dubayah et al. (1990)*

Dubayah et al. (1990) use an atmospheric radiation two stream transfer model, first applied by Dozier (1980) whose solution renders the value of  $K_h$  as

$$K_h = \{ F\downarrow_m + i_0 S_x e^{(-m/i_0)} \} / i_0 S_x \quad \text{-- 17}$$

where  $F\downarrow$  is the downward flux of radiation through the atmosphere,  $i_0$  is the incident angle of  $S_x$ .  $K\downarrow$  on a slope is then found from equation 3. D is calculated by finding a sky view factor which is a function of  $s$ ,  $A_s$ , the angle from the zenith to the horizon, integrating through direction. D is assumed isotropic.  $D_{tr}$  is estimated for each point by calculating an average reflected radiation term and adjusting this by a terrain configuration factor.

These investigators find that the variance and autocorrelation of simulated  $K\downarrow$  depends mostly on sun angle and the elevation grid spacing. However, although variance of radiation decreased with increasing grid size, absolute values of  $K\downarrow$  were found not to vary much when the elevation grid was changed from 25 m to 100 m spacing.

Dubayah (1994) also applied a similar methodology to the Rio Grande river basin. The terrain reflectance,  $D_{tr}$ , is given in this study as

$$D_{tr} = \{(1 + \cos i)/2\} - V_f \quad \text{-- 18}$$

where  $i$  is given by a slightly different expression from that in equation 5 above. The investigator also makes use of radiosonde data and radiative transfer algorithms, such as LOWTRAN7, which are commonly used in remote sensing studies, to estimate the values of some of the atmospheric parameters in equation 18. The model application is grounded by data from pyranometers nearby the study area. Interestingly, pyranometer data after July 1991 recorded a significant fall in values following the Mt. Pinatubo eruption. Semi-variograms for annual and net shortwave radiation values across the drainage basin showed that much of the variability in this area of complex terrain occurred at distances of 300 m or less and almost all of it by 1000m. A similar result would be expected in the Andrews forest area as well. The methodology is applied within a UNIX-based computing framework/environment known as the Image Processing Workbench (IPW) developed by Frew (1990) and currently being revised by Marks (pers. comm., 1995).

*Nikolov and Zeller (1992)*

Nikolov and Zeller (1992) developed a model for estimating monthly  $K\downarrow$  for complex terrain for use in ecological models such as gap models. Their model, while incorporating several empirical approaches, does not depend on parameterization using local site measurements. Their model estimates  $S_x$  using Bonan's approach (equation 15). Atmospheric attenuation is also obtained from an empirical expression employed by Bonan (1988) based on mean monthly cloudiness and three other empirical parameters. They employ an empirical expression for mean monthly cloudiness derived (using data from Bulgaria) from the ratio of mean monthly surface vapor pressure and total monthly precipitation. They then apply an elevation correction formula to allow for the varying elevation of sites for which  $K\downarrow$  is to be estimated. Estimated  $K\downarrow$  is then resolved for S and D using the fraction  $S_h/S_x$  and an empirical

expression for  $D/S$  which is a function of  $S_h/S_x$ . Tilt factors are utilized in order to obtain the values of  $S$  and  $D$  on slopes in relation to their values on horizontal plains. Despite the large amount of empiricism in the method the authors obtain good results when the approach is tested against 69 sets of observations of monthly mean  $K\downarrow$  from a wide variety of stations.

*Fu et al. (1995)*

Fu et al. (1995) produced monthly sums of  $K\downarrow$  and net radiation ( $Q^*$ ) for a 40 year period for a mountainous (39.2 ha) watershed at Parsons, West Virginia. Instead of using individual grid points, they used 432 different terrain segments for their study with a computed  $V_f$  from each facet and a conversion factor for  $S_h$  to  $S$  arriving at the slope.  $S_h$  was computed from equations of the form of, but not identical to, equations 1 and 2. The final equation they used for estimating  $K\downarrow$ , for monthly sums, on a slope was

$$K\downarrow = (S_h - D) R_f + D\{(1 + \cos s)/2\}V_f + D_{tr} \{(1 - \cos s)/2\} \quad \text{--- 19}$$

where  $R_f$  is the conversion factor for converting  $S_h$  to  $S$  on a slope. These investigators obtain a value of  $D$  from long term observed measurements of  $S_h$  and a cloudiness index derived from  $S_h/S_x$  and an empirical expression reported by (Erbs et al. 1982) and which, according to Lu et al., underestimates values of  $D$ . Besides making the estimates of  $K\downarrow$  and  $Q^*$  for the area, Lu et al. conclude that terrain effects on solar radiation become more significant on steeper, north-facing slopes in the winter.

### **Radiation Models Employed at the Andrews Forest**

#### *Hydrology Group*

The Andrews Hydrology Group (Jinfan Duan, Gordon Grant, and Alok Sikka) formulated a stand alone program for simulating shortwave radiation for different slope-aspect combinations and generating these data for times before radiation observations were made at the Andrews (Duan et al, 1994). Their approach is based on the works of Frank and Lee (1966), Swift (1976), Thompson (1976), and Leavesley et al. (1983). The program estimates solar radiation for the given slope-aspect combinations from input data of slope, aspect, latitude, and daily maximum and minimum air temperature. Observed daily  $K\downarrow$  measurements for two years are used to estimate parameters. The program computes potential clear sky radiation for the given slope, aspect, and latitude. Sky cover is estimated as a function of daily range in air temperature. A ratio of measured horizontal surface radiation,  $K_h$ , to potential clear sky radiation (RAJ) is then computed for correcting daily potential solar radiation for the slope-aspect combination (DRAD) of the site.

Daily sky cover (SKY) is computed from the relationship

$$SKY = [ RDM(MO) * (TMX - TMN)] + RDC(MO) \quad \text{--- 20}$$

where RDM is the slope of the sky-cover daily air temperature range for month MO, RDC is the intercept of the sky cover-daily air temperature range for month MO, and TMX and TMN are observed maximum and minimum daily air temperatures. The sky cover value, SKY, is used to compute RAJ by means of the expression

$$RAJ = B + (1-B) * (1-SKY)^P \quad \text{--- 21}$$

where B and P are an empirical values derived from Thompson (1976) with B being a point where the parabola crosses the y axis and P having a suggested value of 0.61. The value of RAJ is adjusted for snow and rain days and an upper limit for it is also specified.  $K\downarrow$  for a slope-aspect combination is given by the product of RAJ and DRAD. The group have refined the method for giving  $K\downarrow$  values for specified time periods less than a day. Daily sunrise and sunset time is based on latitude, longitude, slope, aspect,

and Julian day. D is assumed to be a sine wave between sunrise and sunset with the maximum occurring in the middle of the time period. The amplitude of the wave is computed based on the given radiation during that period. With these assumptions total daily  $K\downarrow$  can be partitioned to any desired time interval based on amplitude and time.

This methodology does not resolve S and D although it implicitly takes them into account to some extent through the use of sky cover.

#### *Bioclimate Group*

The bioclimatology group (Ron Neilsen, Ed Llewellyn) undertake studies which extend beyond the Andrews Forest. They use solar radiation input for further studies and estimates of photosynthesis and potential evapotranspiration rates. This group primarily uses  $K\downarrow$  estimates from the IPW system (see under Dubayah et al. 1990 above). They use a 15 m resolution for their grid. The bioclimatology group also uses the model of Nikolov and Zeller (1992).

#### *Gap Modeling Group*

This group is led by Mark Harmon, with Barbara Marks being the head programmer. The group needs solar radiation data, as well as monthly potential evapotranspiration rates, detritus drying rates, and sun angles as input for ecological forest gap models. They primarily use the IPW approach with a 30x30 m grid. They also use another program called SolarRad which operates on a grid basis and follows the approach of Bonan (1989). The approach seeks to estimate actual, as opposed to potential, radiation and thus estimates monthly mean cloud cover from temperature ranges and the amount of precipitation. Transmissivity is estimated (after Nikolov and Zeller, 1992) as a function of latitude, elevation, and mean monthly cloud cover. Partitioning of  $K\downarrow$  into S and D and adjusting for the tilt of a slope is done also following Nikolov and Zeller (1992).

#### *Miscellaneous Studies*

At least two important microclimate studies at the Andrews Forest have included short term measurements of solar radiation.

Tom Spies and Andrew Gray made measurements between February 1991 and December 1992 on the north edge, south edge, and center of deliberately formed forest gaps (one in the Andrews and three at Wind River). Photosynthetic photon flux density (PPFD) was measured at 1.5 m. height with 10 sec observations integrated over 2 hr periods. Mobile temporary stations were also used.

Jiquan Chen measured  $K\downarrow$  at the HJA in relation to forest edge microclimate measurements performed also at Wind River (Chen et al. 1993).

Other important studies completed in other areas of the Pacific Northwest should also be noted.

Scatterlund and Means (1979) used an empirical equation which included resolution of  $K\downarrow$  into S, D, and the radiation scattered through clouds estimated from cloud cover values, to produce monthly mean maps of  $K\downarrow$  for Oregon. Their estimated values agreed well, in all season, with observed measurements.

One of the few studies to actually use measurements (albeit short term) of  $K\downarrow$  and  $Q^*$  with instruments parallel to the slope in question was that of Holbo and Childs (1987). These investigators noted the higher values in  $K\downarrow$  and  $Q^*$  values over clearcut as compared to shelterwood surfaces in complex terrain in southwest Oregon. They also observed a significant lowering of the albedo from unburned (0.21) to burned (0.13) sites. A somewhat more comprehensive endeavor to measure mostly

$K\downarrow$ , and occasionally  $D$ , across Oregon took place around the early 1980s organized by the University of Oregon Solar Radiation Laboratory (1983).  $K\downarrow$  was also measured for a period of about two years in the early 1990s at the five sites in the Oregon Transect Ecosystem Research Project (OTTER) (Glassy and Running, 1994).

## Discussion

A number of points arise from this review. First, it seems that there has been a certain amount of isolation among the various disciplines which have contributed to the modeling of solar radiation. Workers in the disparate fields have been naturally more familiar with the models used in their fields rather than those from other disciplines. Different disciplines emphasize different aspects of the overall topic. Architects and engineers, for example, are not so interested in spectral models as are remote sensors and ecologists. The interest in spectral models is increasing and although this is a difficult topic, some important advances are being made. Yang and Miller (1995), for example have provided a useful model which estimates global irradiance in five broad and significant spectral bands. Second, there seem to be differences in approaches to making estimates of solar radiation receipt in different parts of the world as well. The approach in North America is almost entirely based on theoretical models while the approach in Europe, as judged by the work of the Commission of European Communities (Dogniaux, 1995), seems to be more empirically based. Third, the theoretical approach is further divided between studies based on grid points of the area in question and studies which deconstruct the area into a number of explicit slope facets. Fourth, the process of modeling potential shortwave radiation in complex terrain is one in which a continuum of approaches may be taken ranging from those which simply compute  $S$  to those which also estimate  $D$  with a variety of degrees of sophistication. Similarly, the effect of the surrounding terrain on shading and reflection of  $S$  and  $D$  may be taken into account with different levels of accuracy. Duguay (1993) points out that the main differences between many of these models is found in the way in which they treat  $D$  and  $D_{tr}$ . Most models seem to recognize the importance of treating isotropic/anisotropic conditions although none of them has been tested against real data over a range of geographic and environmental conditions. Seldom do models incorporate more than first order effects related to  $D_{tr}$ . Duguay points out that a complete treatment of  $D_{tr}$  would need to include 1) the exposure of surrounding terrain slopes, 2) the distance between the point of interest and the contributing points, 3) the orientation of the point in question to other visible topographic points, and 4) the albedo of the surrounding terrain. Duguay notes the existence of a trade off between potentially increased accuracy and computational efficiency. Fifth, the incorporation of the effects of clouds into the modeling process presents a whole added layer of complexity not treated in this review. The availability of observed information for model parameters, such as atmospheric transmissivity and absorption by ever varying quantities of aerosols is another factor that may influence the choice of a modeling approach. Sixth, Dubayah (1994) further points out that there is another level of detail which radiation models of the kind discussed here usually omit. This level of detail concerns the geometry of the vegetation morphology both at the level of the individual plant and at the level of its components such as leaves and needles. This level of detail is being studied in remote sensing investigations but, as might be expected, it is a difficult one to treat. Finally, available computational resources and the availability of required computer code, also play a role in model selection.

## The Williams Model

The model selected for use in the present study is that developed by Larry Williams (Williams et al. 1972). The reasons for making this selection will now be discussed.

The foregoing review demonstrates that there are some basic similarities in models for estimating  $K\downarrow$  particularly in the equations and algorithms used to estimate  $S$ . However there are major differences in subsequent steps especially in the following areas:

- 1) The treatment of atmospheric attenuation,
- 2) estimation and inclusion of  $D$  and  $D_{tr}$ ,
- 3) use of grids or slope facets to describe the topography,
- 4) the incorporation or not of shading by topography and the way in which any incorporation is performed.

Each investigator is faced with the decision on how to treat these four issues. The decision is made after considering the amount of input data available, the degree of detail and accuracy required, computation resources available, and the ease with which a modeling system may be used by others. Even more important is the purpose for which the modeling is performed. Dubayah (1994) points out that there are two primary classes of use for the kinds of radiation models reviewed above. First is to use modeled  $K\downarrow$  as a direct explanatory variable for spatial distribution of biophysical phenomena such as vegetation distribution. The second use is for driving other functional models such as those for estimating evapotranspiration or primary productivity.

The goal of the present study emphasizes the investigation of spatial distribution rather than the provision of data for functional models, although the latter is by no means precluded. This study aims to examine the changing geography over the annual period of potential solar radiation input into the area of the Andrews Forest and to identify locations of special interest and possible *spatial* relations with other biophysical phenomena. It is in this context that the Williams model has been selected for use.

The advantages and disadvantages of the Williams model should be noted. There are several advantages. The model is based on the generally accepted algorithms for computation of  $S$ , and to a certain extent,  $D$ . It incorporates the effects of shading at a point by surrounding topography. It is grid based and so does not require pre-analysis of slope facets. The selection of grid density has a certain amount of flexibility. The model is quite portable from one investigator to another and adaptable for use on microcomputers. The model may be easily used for any area for which digital elevation data can be obtained. The model has been tested against real data for mountain situations in Canada and has found to function accurately (Munro and Young, 1982). There are also some disadvantages related to use of the model. It does not take into account terrain reflectance. Its application to a large geographic area at a fine grid density would, in most cases, not be possible on a microcomputer without a complete restructuring of its input-output system. Calibration of the model requires the use of observational data which then renders this data unavailable for assessing the accuracy of the model output.

Despite these disadvantages, many of which apply to many other models as well, given overall consideration of both theoretical and practical factors, and particularly the purpose of application, the Williams model was selected as appropriate for use in this study.

## PROCEDURE

### Overview

Initial work was performed using ERDAS software on test digital elevation model (DEM) data. The algorithm based on the work of Williams et al. (1972) was selected and adapted for use on current PC systems. The adapted and modified computer program was called ANRAD. SURFER software was employed to produce maps of both the Andrews topography and the output radiation values. Following initial testing, the standard base Andrews DEM data set was obtained and processed for input into ANRAD. Observed radiation data from the Primary Meteorological and Vanilla Leaf observation stations at the Andrews Forest were used to obtain the best estimate of atmospheric transmissivity values for calibration of, and input into, the ANRAD program. The program was then used to obtain estimates of potential direct and diffuse radiation at 120 m resolution grid for the Andrews area for the days of interest (target days) during the year.

## **Preliminary steps**

Most GIS, and much other related ecological work, is performed at the PNW Forestry Sciences laboratory using ERDAS software in a UNIX environment. Consequently, in order to maximize compatibility, initial steps in this research were made using the micro-computer, PC, version of ERDAS version 7.5. Test digital elevation model (DEM) data for the Andrews area were provided by Dr. Warren Cohen in the form of ERDAS LAN files. Eventually, most of the work for this project was performed outside the ERDAS environment but relevant procedures using this environment are discussed for the benefit of future workers who may be interested. Note, however, that ERDAS 7.5 is in the process of being superseded by a version called ERDAS IMAGINE.

After selecting the Williams et al. (1972) algorithm, the original program for this algorithm was adapted for use on current PC systems. Required code changes were made to convert between Minnesota FORTRAN and Microsoft (MS) FORTRAN 5.1. The main changes involved input output features and the modification of the program to use larger data matrices than originally employed. The modified program was called ANRAD and various versions thereof, each one being indicated by a number at the end of the word ANRAD. The output from ANRAD was tested against the output for an independent potential radiation estimation program developed by Fuggle (1970) to check for compatibility. A data set for a flat plain near sea level was developed for ANRAD to perform the compatibility tests. The results from the two programs for direct radiation daily total at the winter solstice and 40° N were similar to within 0.13 MJ/sq. m/day (3.0 ly). This is acceptable accuracy to permit confidence with the use of the ANRAD program.

## **Data Preparation**

The ANRAD program can be applied to any limited set of DEM data. Restrictions on the size of the data set are discussed below. The following steps are required to construct the elevation data matrix.

- 1) Remove any header information the file might have but keep a note of this information for later use.
- 2) Adjust the data set to a small enough size so that the ANRAD program will operate on a PC of a given size RAM (See notes in Appendix 4, Background section). If the data set is too large, degrade the set by systematically removing data points either by using the ERDAS Version 7.5 program DATATAB, or equivalent, or by using the SKIP program discussed in Appendix 2.
- 3) SURFER for WINDOWS version 6 is used in this study for creating maps of the potential radiation values. Some earlier versions of SURFER will also work. Output data from ERDAS DATATAB or from SKIP need to be adjusted to reverse the rows of DEM data for use in ANRAD and SURFER. The adjustment is necessary because the DEM and ERDAS data sets and programs implicitly operate from the top left hand side of the data matrix while ANRAD and SURFER explicitly start work at the bottom left hand side of the matrix. The adjustment is made with the ELDAT program detailed in Appendix 3.
- 4) A slight modification of the ANRAD program (named ANRAD4E) produces a reduced size elevation matrix for use with SURFER for making a topographic map which is directly compatible with the output radiation maps. The reduced data size is required because ANRAD needs a data set two data rows and columns larger than the output radiation data set so that it can compute areas of possible shading near the edges of the map. ANRAD4E provides the required reduced size elevation matrix for the production of a SURFER map compatible with those eventually produced from ANRAD output. Some of the output files of matrix information already have SURFER headers attached by the program which produced them. These files are specified in the appendices and need to have .GRD suffixes added to their names for direct entry into the SURFER Map routine.

To summarize, the following steps are used for data preparation:

- 1) Obtain DEM data
- 2) Use SKIP, or equivalent, to reduce the size of the data matrix for use by ANRAD and SURFER.
- 3) Use ELDAT to reverse the rows of elevation data. This produces an output file called ELEVDATA which must be renamed ANDAT3 to be used as elevation input for ANRAD.
- 4) Use ANRAD4E to provide a reduced size elevation matrix for the production of a SURFER map compatible with those eventually produced from ANRAD output.

Much of the input data for ANRAD (Appendix 4), such as latitude and Julian day, is straightforward to collect or is provided as default by the program. However, an appropriate value for atmospheric transmissivity is more complicated to obtain and is discussed here following consideration of the observed radiation at the Andrews Forest.

### Observed Radiation Data at the Andrews

Shortwave radiation receipt has been observed at two of the current four benchmark observing stations at the Andrews Forest. The stations are called Primary Meteorological Station (Primet) (elevation 426 m, lat. 44° 15', lon. 122° 10') and Vanilla Leaf (elevation 1267 m, lat. 44° 16', lon. 122° 08'). The two other benchmark stations, Upper Lookout and Central Meteorological Station, began recording radiation in 1995. Data for the year 1994 from the first two stations is used in this study. Radiation is measured at these stations with a Kipp and Zonen radiometer system which includes a CM5 thermopile and a model CM3 pyranometer. Daily totals of  $K\downarrow$  for the year are shown in Figs. 4 and 5. The data, which have not been corrected in this study for days of dubious values, show that Vanilla Leaf receives significantly more radiation than Primet. This is because of the latter's position in a steep sided valley. The figures also show the effect of relatively cloud-free conditions in the summer time and the very few days of maximum potential radiation in the other three seasons. Winter data are often questionable, particularly at Vanilla Leaf, because of the possibility of snow covering the sensors.

### Estimation of Atmospheric Transmissivity

An operational value for atmospheric transmissivity ( $p$ ) applicable for clear skies would be 0.84 (Oke, 1987 p. 345). Oke quotes the cloudless sky atmospheric transmissivity value as varying from 0.6 in smog and haze to 0.9 in very clear conditions. It was decided to employ data observed at the Andrews to arrive at a reasonable estimate of  $p$  for the location. Estimates of TOA radiation ( $S_x$ ) at the site for different times were made using equation 3 for daily total values. These estimates correspond well to monthly means given by (Iqbal, 1983 p. 67) for latitude 45°N. Data used in the procedure for estimating  $p$  are shown in Appendix 5. Orbital radius vector and solar declination data for these computations were obtained from *The Astronomical Almanac for 1994* (Government Printing Office, Washington, DC). Observed values of  $K\downarrow$  at Primet and Vanilla Leaf were adjusted for shading and for cloud cover for the dates used in this study. All calculations were made for both stations but the  $p$  values finally chosen were those for Vanilla Leaf since it was believed that they were the most accurate. This was especially so for the winter period when the Primet site suffers severely from shading. Adjustments for shading were made in the following manner. First, angles of the local horizon above the horizontal plane were measured at 10° compass direction intervals for both the Primet and Vanilla Leaf recording sites. These data were then plotted onto a chart of solar paths through the sky for various dates during the year (List, 1951. p. 502). It was then possible to estimate the hours when the site was shaded from direct radiation on the target dates used in this study. A version of the Garnier and Ohmura (1968) method of estimating radiation receipt was employed using the program by Fuggle (1970). This program gives the amount of radiation in hourly increments arriving at the specified site and date. The percentage of radiation lost at the site by shading was estimated by subtracting the radiation receipt estimated by the Fuggle program for the times when the solar path diagrams showed the site to be in shade. The operational value of transmissivity, 0.84, described above was used in this exercise. Second, cloud free values of observed

### PRIMET GLOBAL RADIATION 1994

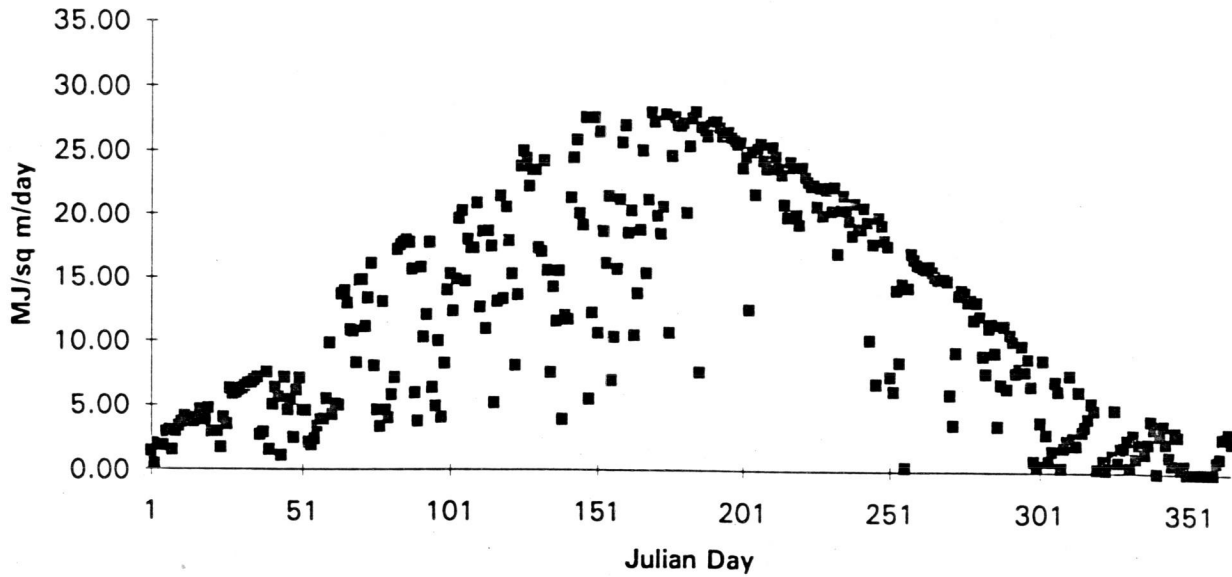


Fig 4. Daily totals of shortwave radiation at the Primary Meteorological Station, 1994.

### VANILLA LEAF GLOBAL RADIATION 1994

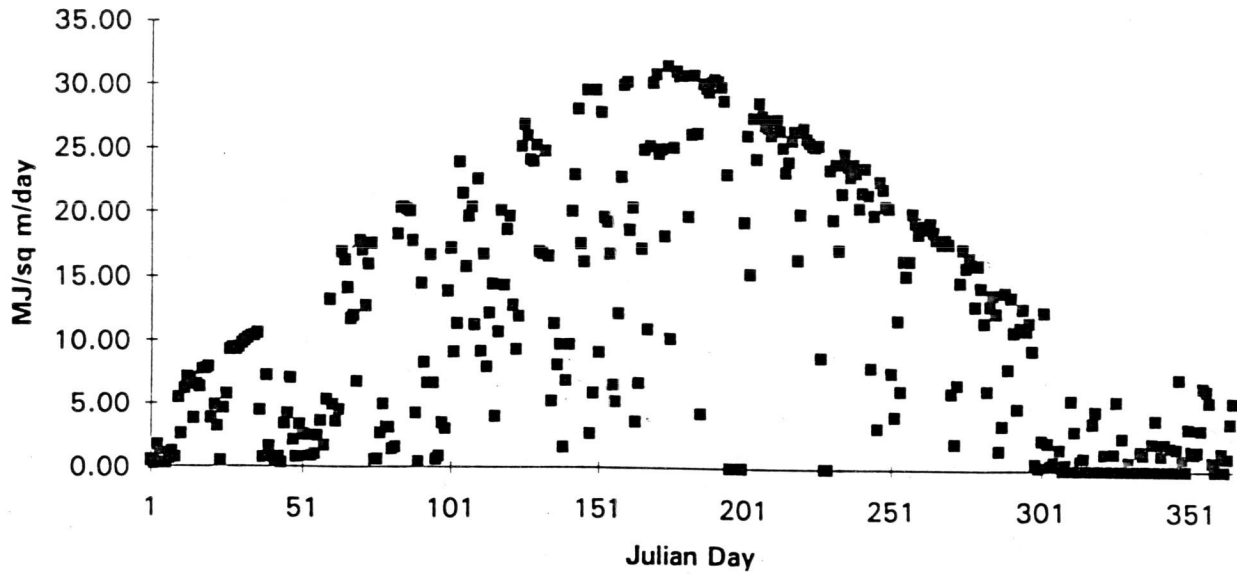


Fig 5. Daily totals of shortwave radiation at Vanilla Leaf Station, 1994.

radiation for the target dates were required. These were obtained by plotting out daily values of radiation recorded at the two sites for 1994 (Figs. 4 and 5). It is possible to estimate what the radiation value would be on any particular date by extrapolation from the maximum values indicated on these plots. The daily data were plotted out on three separate graphs of 120 days of data each to obtain greater accuracy for the extrapolations. Third, having obtained estimates of the amount of radiation potentially arriving at the sites on a cloudless day on the target dates, the resulting values were adjusted to what they would have been if the sites were not shaded. Finally, the estimated  $S/S_x$ , which represent the required transmissivity (p) values were calculated. The values of p obtained in this manner for the appropriate dates were Dec. 21, 0.68, March 21, 0.68, June 21, 0.78, Jan. 15, 0.69, Feb. 14, 0.74, April 15, 0.72, May 15, 0.74. The transmissivity values estimated using the foregoing procedure are similar to the 0.68 value measured at Eugene between 1980 and 1982 (University of Oregon Solar Radiation Laboratory, 1983), and are consistent with the sea level value of 0.60 used in the Oregon study of Glassy and Running (1994). Glassy and Running (1994) increased the value above 0.60 with elevation above sea level. Transmissivity estimates made in the way described are only approximations since, besides having possible errors at each stage of the computation, they effectively give the ratio of  $(S+D)/S_x$  instead of  $S/S_x$ . However these data are believed to be of more value than would be obtained by assuming a standard value from the literature for each target day. An approximation for resolving S and D was made by running the ANRAD program with the operational transmissivity value and comparing the grid average S and D values for the target dates and acquiring an approximation for the  $S/(S+D)$  ratio from which "unshaded" values of S, and transmissivity values, were obtained. An independent check on the resulting p values was made by entering them into the Fuggle (1970) program for the target dates and using the estimated  $S/(S+D)$  ratios to recalculate the "observed unshaded" S+D values. This exercise showed that more realistic values of p, for this location, could be obtained from  $(S+D)/S_x$  rather than  $S/S_x$ . Selected computations for establishing p values are given in Appendix 5.

### Application of ANRAD

The application in this study used data applicable to the H. J. Andrews Forest. The data includes: Latitude 44° 12' N and atmospheric transmissivity as described above. Default data were used for values of the fraction of extraterrestrial radiation absorbed in the atmosphere, and the fraction of scattered radiation scattered downward. The program was run for Dec 21 (Winter Solstice - JD 355), March 21 (Spring Equinox - JD 80), June 21 (Summer Solstice - JD 172) and for mid month dates Jan 15 (JD 15), Feb 14 (JD 45), April 15 (JD 105), May 15 (JD 135) in order to give a representative picture of seasonal change. Data for the months in the second half of the year, when the sun gradually becomes lower in the sky, will be a mirror image of that estimated for the first half of the year. Test elevation data were in m and were spaced at 125 m intervals. These data were supplied by Dr. Warren Cohen. Final data, also in m, were run at an interval of 120 m and were supplied by Ms. Barbara Marks in August 1995 and represent the "base" Andrews DEM data which is used in the Andrews GIS Atlas. These data (File name BASEDEM in this report) have 30 m cells with 343 rows and 457 columns. They are from UTM zone 10 (see appendix 1) and have the following UTM coordinates: xmin 558365, ymin 4893415, xmax 572075, ymax 4903705. They were reduced to 86 rows and 115 columns with 120 m spacing for use in ANRAD.

### THE POTENTIAL RADIATION MAPS

Potential radiation (PR) maps were produced for the area of, and adjacent to, the H. J. Andrews Experimental Forest using the procedures described above. Although data for both direct radiation and diffuse radiation were produced, only the maps for the sum of direct and diffuse radiation are discussed here since these are the closest representation to reality. Individual PR maps, the series of PR maps, and some possible relations between the PR distributions and distributions shown on other data layers of the Andrews GIS Atlas will be discussed.

## Individual Maps

Examination of a PR map without shaded infilling of the various isolines (Fig. 6) immediately indicates the great spatial variability of daily total PR values across the Andrews area as well as some areas where there are very steep gradients of PR values. In order to appreciate the amount of detail it was found more effective to present the PR maps with a shaded infill between individual contour lines. A series of such maps is presented for Dec. 21 (Fig. 7), Jan. 15 (Fig. 8), Feb. 15 (Fig. 9), Mar. 21 (Fig. 10), April 15 (Fig. 11), May 15 (Fig. 12), and June 21 (Fig. 13). A transparent overlay showing the contour lines and perimeter of the Andrews (a copy of Fig. 2) is provided in a pocket at the end of this report for use with the individual PR maps.

It is most instructive to look first at the PR map for June 21 (Fig. 13). This represents conditions during the growing season for the ecosystem. Also it should be noted that at this time of the year, when rainstorms are less frequent and skies are more free of clouds, the actual radiation values will come close to the potential radiation values. Here one sees the steep radiation gradients once more. These areas might be expected to have some influences on other biophysical spatial distributions and would be worthy of close attention in the field. The areas of steep radiation gradients include: 1) the N to NE side of Lookout Mountain particularly near its top and at its base near Lookout Creek, 2) the N side of Lookout Ridge near the ridge line, 3) the SE side of McRae Creek valley, and 4) near the top of the ridge running from Frisell Point to Carpenter Mountain. There are also some steep radiation gradients to be found in the land areas outside the Lookout Creek watershed both to the NW and to the E. Steep radiation gradients were also a feature of the application of a similar modeling system to the Peyto Glacier in Alberta, Canada (Munro and Young, 1982).

In addition, use of the contour overlay demonstrates the following characteristics only the first of which is immediately intuitively obvious:

- a) As expected, areas of highest PR are on south facing slopes and vice versa.
- b) The south facing slopes which have the highest PR tend to be at the higher elevations in the Andrews. This is due to the fact that the lower elevation areas in the SW of the Andrews tend to be in relatively steep sided and therefore shaded valleys. This has implications for studies at the Andrews because a large number of studies, particularly the earlier ones, were performed in the lower elevation watersheds. Many observational data sets, such as climate for example, are under-represented at the higher elevation areas.
- c) Even at the 120 m resolution, and even in the period of high sun of summer, there is a large amount of spatial heterogeneity in PR values. Each small sub-creek and sub-watershed has its own considerable variation in PR values. Although not included in the calculations, the presence or absence of tall trees will greatly increase this heterogeneity. A landscape composed of forest patches and clear cuts creates its own 'topography' which is superimposed on the natural land forms. The local horizons measured at Primet and Vanilla leaf would have been very different if their cutting and regrowth histories had been different. As mentioned in the general description of the climate the predominant trees in the Andrews Forest are very tall when mature. Consequently, actual measurements of  $K_{\downarrow}$  in forest gap studies such as those of Spies and Gray (see above) are particularly important.
- d) As a coarse geographical classification for the June 21 PR values, the Andrews Forest could be divided into two areas roughly separated by the stream bed of Lookout Creek. North of the creek, with the exception of the slopes to the SE of McRae creek, is an area of relatively high PR values exceeding  $34 \text{ MJ/m}^2/\text{day}$ . South of Lookout Creek is an area of relatively low PR usually less than  $34 \text{ MJ/m}^2/\text{day}$ .
- e) The climate station at Vanilla Leaf is well exposed and will be able to record the maximum, or close to the maximum, amount of  $K_{\downarrow}$  at a horizontal surface at any point in the Andrews. The Primary

Fig 6. Potential direct and diffuse radiation over the H. J. Andrews Experimental Forest for June 21 presented without the infilling of isolines.

Fig 7. Potential direct and diffuse radiation over the H. J. Andrews Experimental Forest for Dec 21.

Fig 8. Potential direct and diffuse radiation over the H. J. Andrews Experimental Forest for Jan 15.

Fig 9. Potential direct and diffuse radiation over the H. J. Andrews Experimental Forest for Feb 15.

Fig 10. Potential direct and diffuse radiation over the H. J. Andrews Experimental Forest for Mar 21.

Fig 11. Potential direct and diffuse radiation over the H. J. Andrews Experimental Forest for April 15.

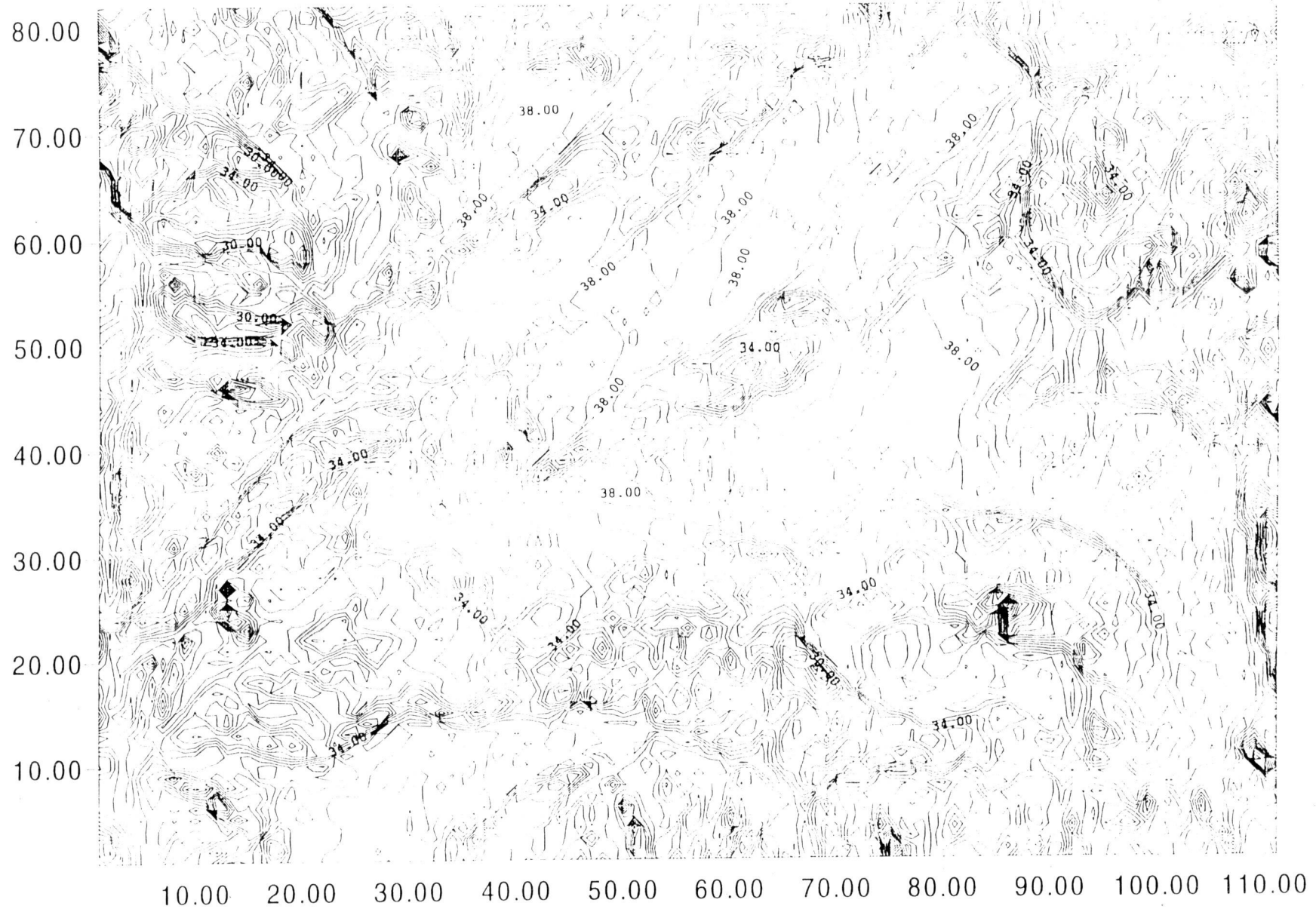
Fig 12. Potential direct and diffuse radiation over the H. J. Andrews Experimental Forest for May 15.

Fig 13. Potential direct and diffuse radiation over the H. J. Andrews Experimental Forest for June 21.

Back Folder      Transparency copy of Fig. 2 for overlaying on Figs. 7 - 13.

# POTENTIAL DIRECT AND DIFFUSE RADIATION

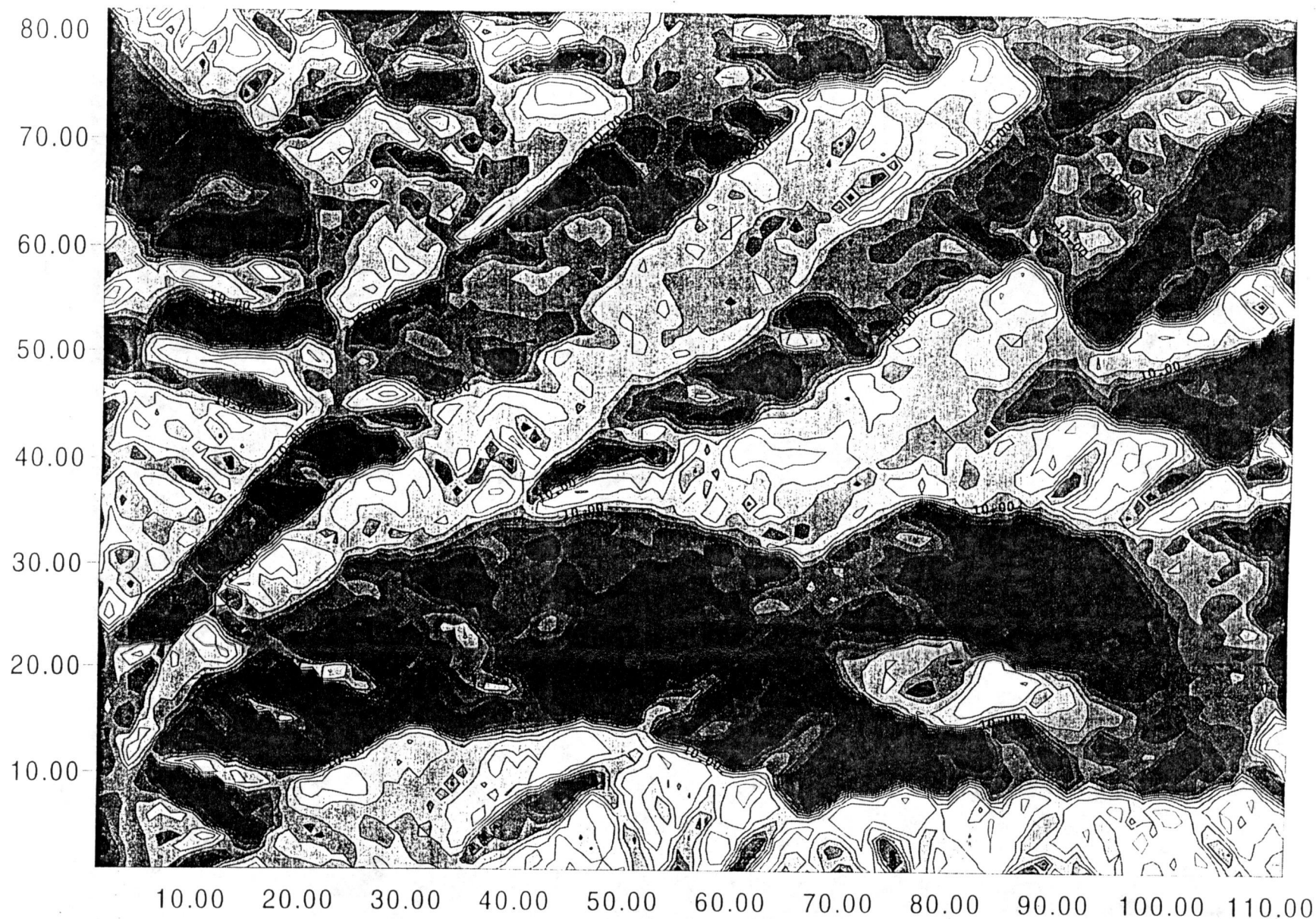
JUNE 21



Axis units are 120 m (e.g. 10 = 120x120 m from lower left hand corner of the map)  
North is to the top of the map. Isolines are in MJ/sq.m/day. Isoline interval is 1 MJ/sq.m/day.  
Highest and lowest isoline values are 38 and 17 MJ/sq.cm/day respectively.

DEC 21

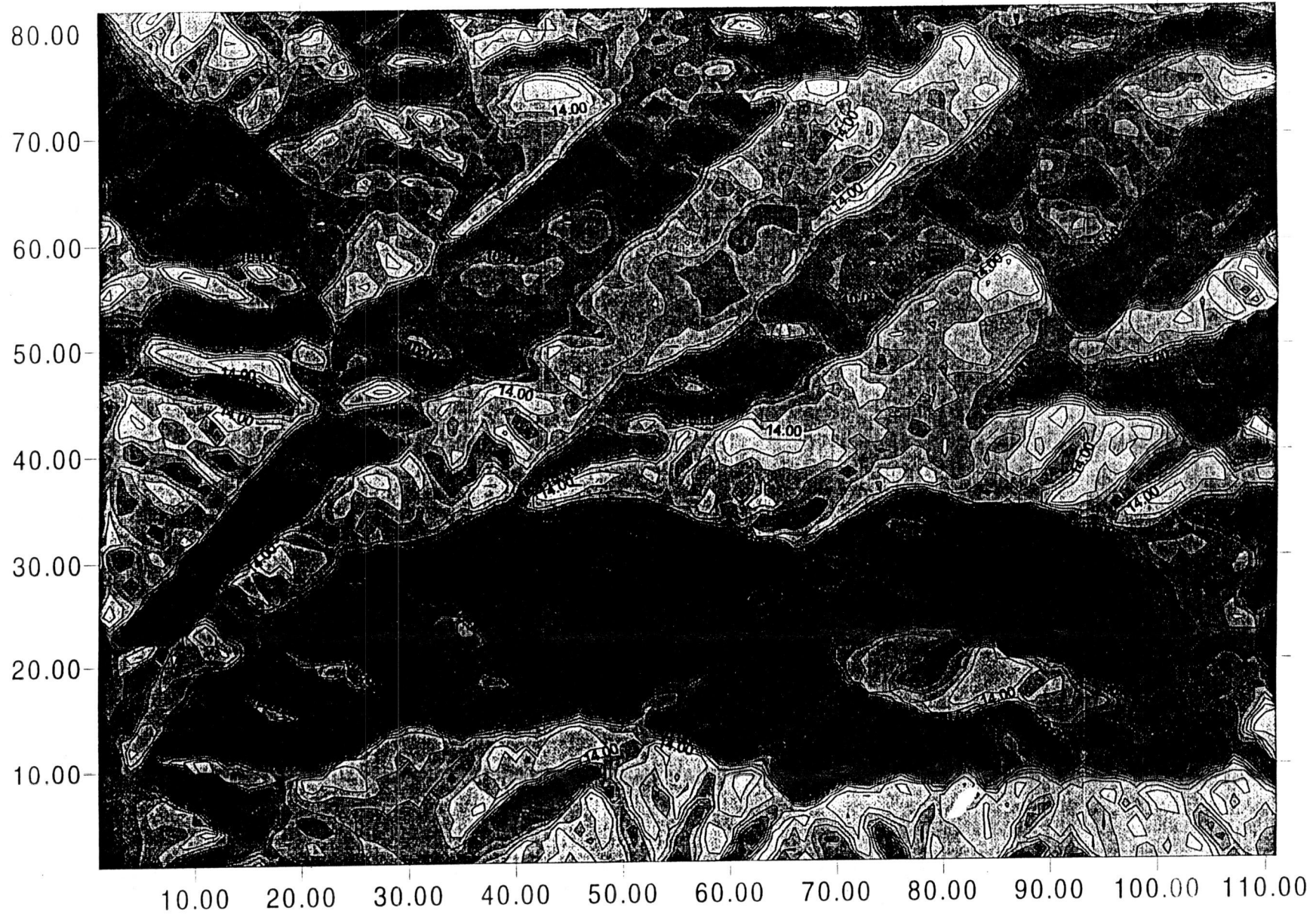
# POTENTIAL DIRECT AND DIFFUSE RADIATION



Axis units are 120 m (e.g. 10 = 120x120 m from lower left hand corner of map)  
North is to the top of the map. Isolines are in MJ/sq.m/day. Isoline interval is 1 MJ/sq.m/day.  
Highest and lowest isoline values are 14 and 5 MJ/sq.m/day respectively.

# POTENTIAL DIRECT AND DIFFUSE RADIATION

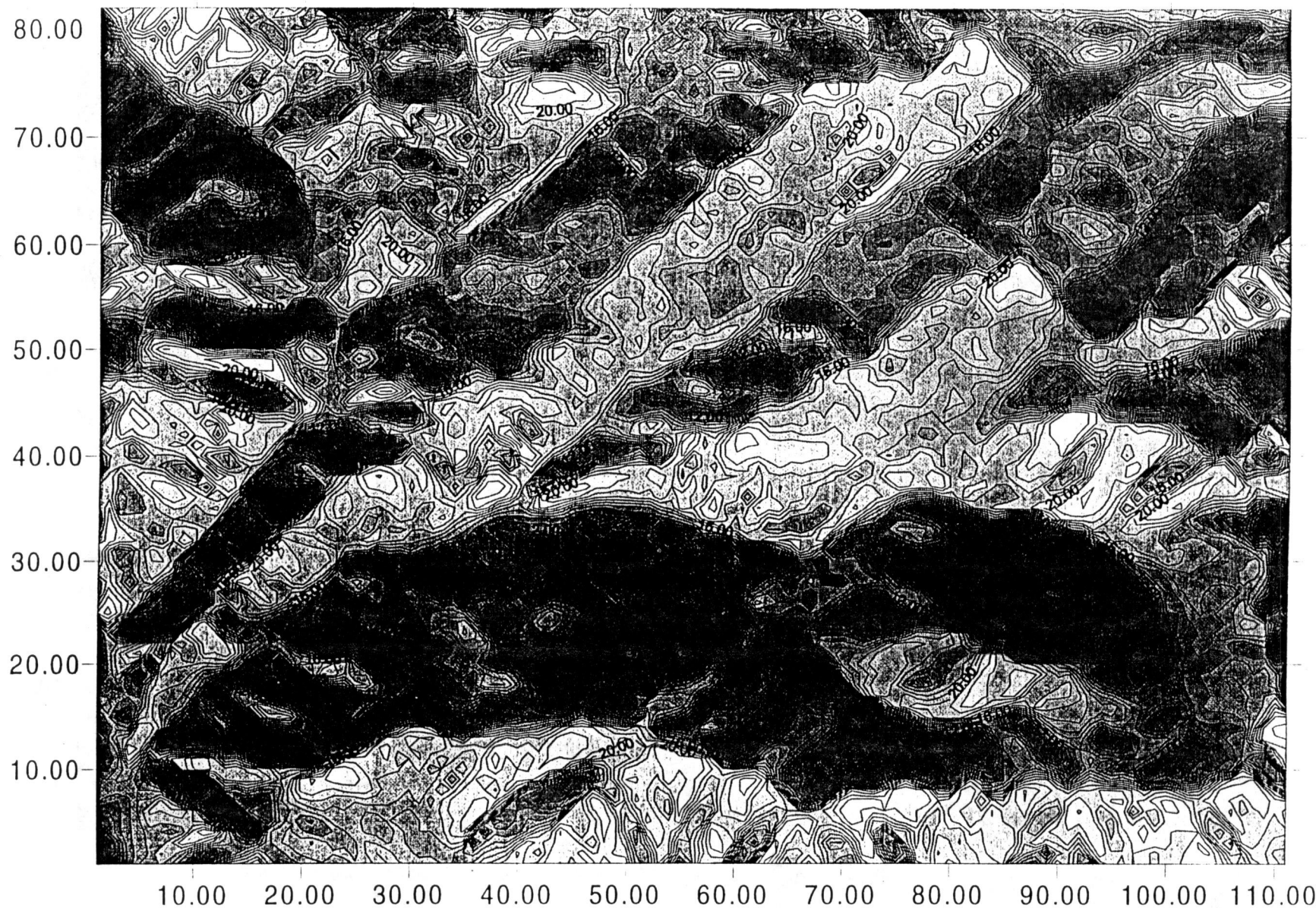
JAN 15



Axis units are 120 m (e.g. 10 = 120x10 m from lower left hand corner of the map)  
North is to the top of the map. Isolines are in MJ/sq.m/day. Isoline interval is 1 MJ/sq.m/day.  
Highest and lowest isoline values are 18 and 5 MJ/sq.m/day respectively.

FEB 15

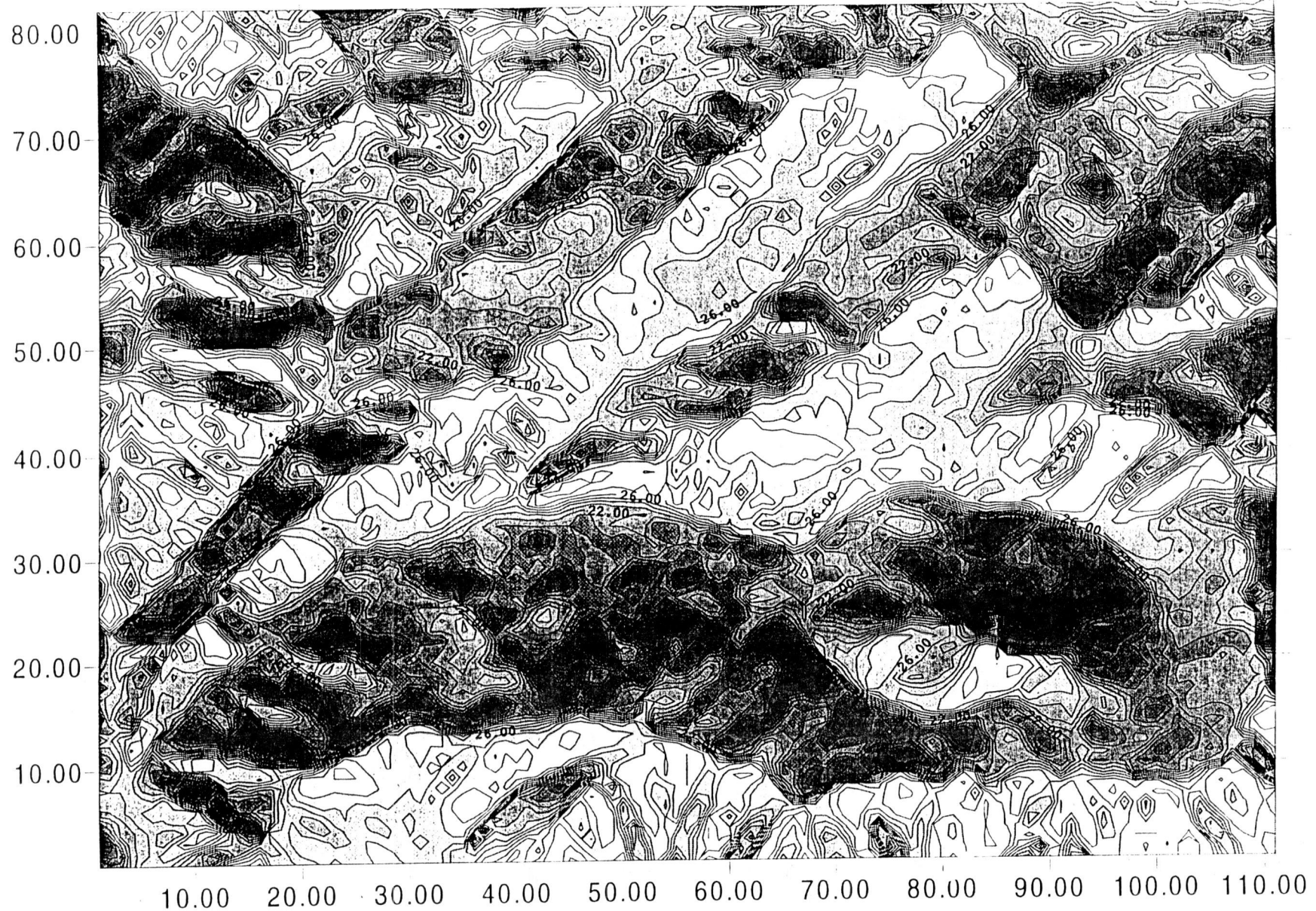
# POTENTIAL DIRECT AND DIFFUSE RADIATION



Axis units are 120 m (e.g. 10 = 120x120 m from lower left hand corner of map)  
North is to the top of the map. Isolines are in MJ/sq.m/day. Isoline interval is 1 MJ/sq.m/day.  
Highest and lowest isoline values are 24 and 4 MJ/sq.m/day respectively.

# POTENTIAL DIRECT AND DIFFUSE RADIATION

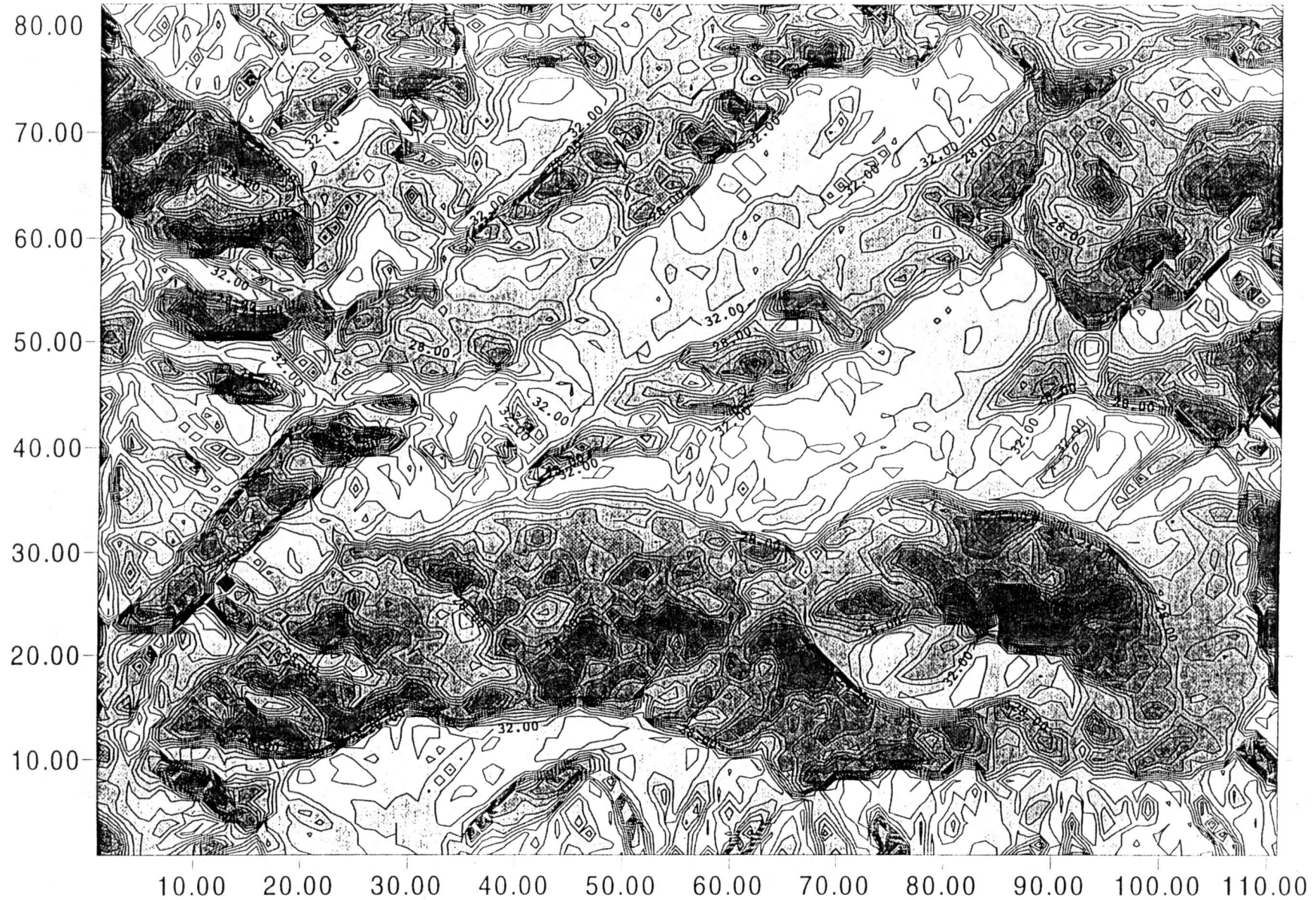
MAR 21



Axis units are 120 m (e.g. 10 = 120x120 m from lower left hand corner of map)  
North is to the top of the map. Isolines are in MJ/sq.m/day. Isoline interval is 1 MJ/sq.m/day.  
Highest and lowest isoline values are 29 and 10 MJ/sq.m/day respectively.

APRIL 15

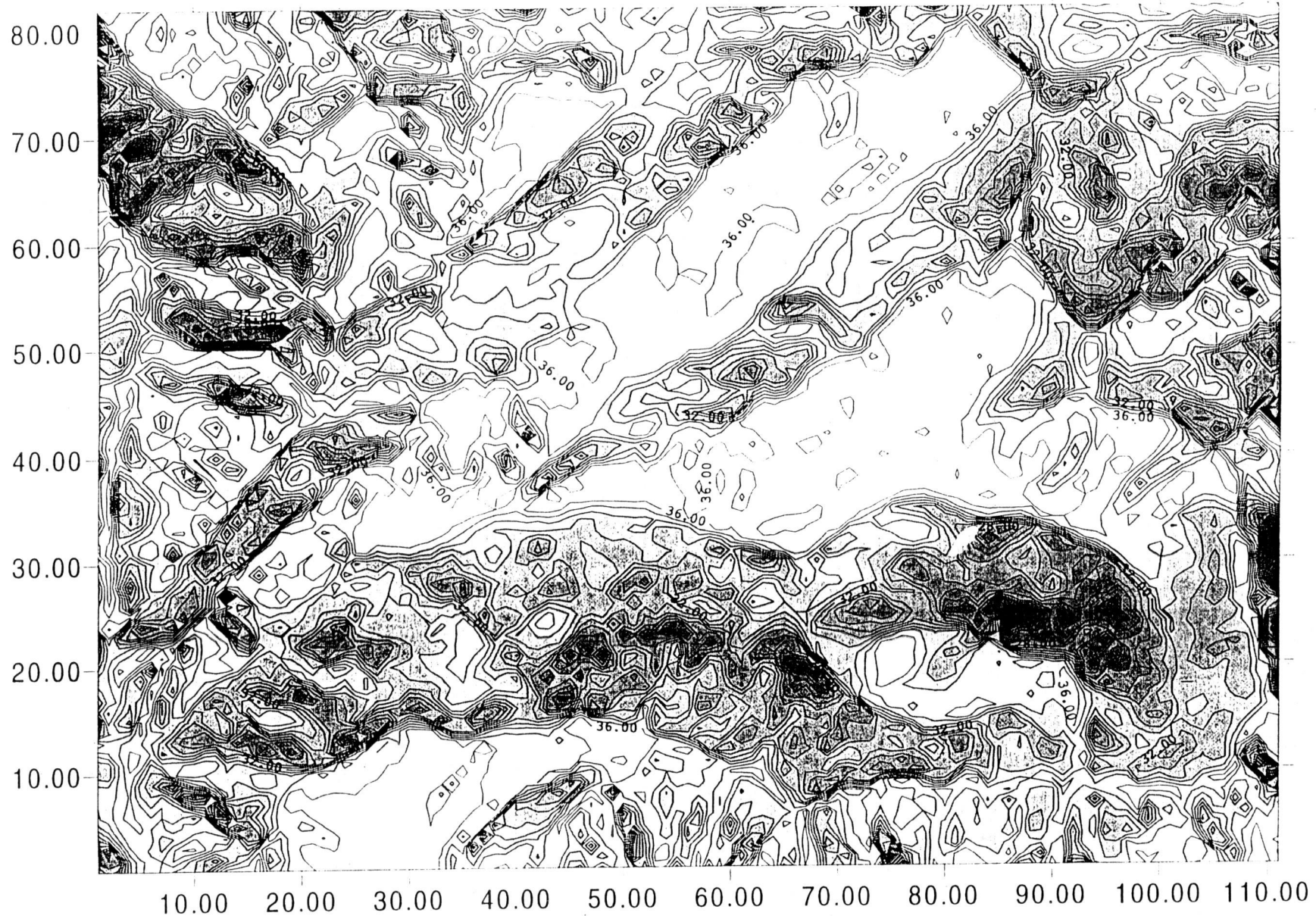
# POTENTIAL DIRECT AND DIFFUSE RADIATION



Axis units are 120 m (e.g. 10 = 120x120 m from lower left hand corner of map)  
North is to the top of the map. Isolines are in MJ/sq.m/day. Isoline interval is 1 MJ/sq.m/day.  
Highest and lowest isoline values are 33 and 13 MJ/sq.m/day respectively.

# POTENTIAL DIRECT AND DIFFUSE RADIATION

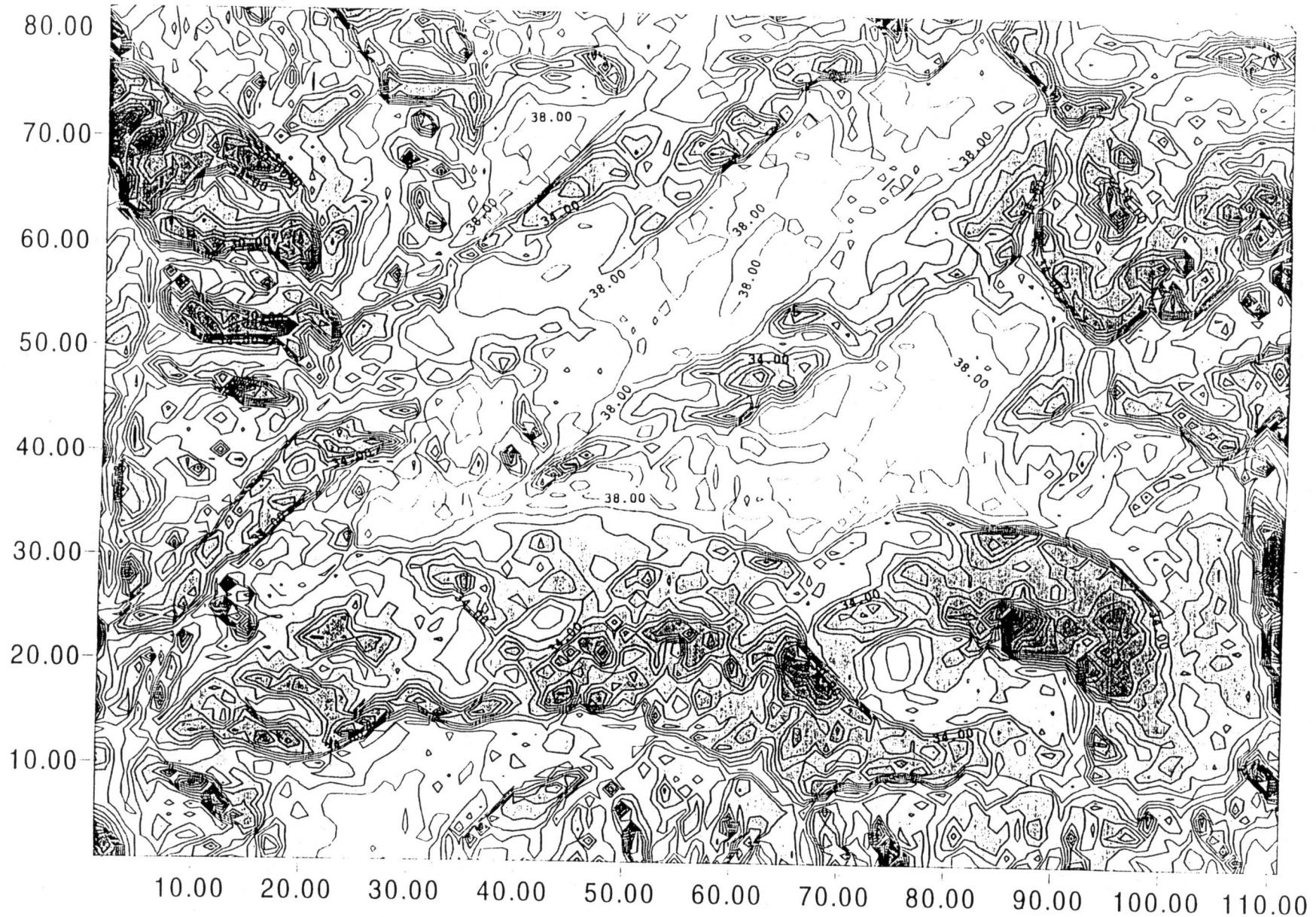
MAY 15



Axis units are 120 m (e.g. 10 = 120x120 m from lower left hand corner of the map)  
North is to the top of the map. Isolines are in MJ/sq.m/day. Isoline interval is 1 MJ/sq.m/day.  
Highest and lowest isoline values are 36 and 17 MJ/sq.m/day respectively.

JUNE 21

# POTENTIAL DIRECT AND DIFFUSE RADIATION



Axis units are 120 m (e.g. 10 = 120x10 m from lower left hand corner of the map)  
North is to the top of the map. Isolines are in MJ/sq.m/day. Isoline interval is 1 MJ/sq.m/day.  
Highest and lowest isoline values are 38 and 17 MJ/sq.cm/day respectively.

Meteorological Station, on the other hand, is poorly exposed. Indeed, at the winter solstice, Primet is almost totally shaded by trees and topography.

The PR map for Dec. 21 (Fig. 7), the time of the winter solstice, shows:

- a) There is a similar fundamental, topographically-anchored pattern of PR but there are far less extreme variations in the absolute values. Note that for Dec 21 the highest and lowest isolines have values of 14 and 5 MJ/m<sup>2</sup>/day respectively, a difference of 9 MJ/m<sup>2</sup>/day compared to the June 21 case of 38 and 17 MJ/m<sup>2</sup>/day, a difference of 21 MJ/m<sup>2</sup>/day.
- b) Consequently, although the areas of steep PR gradients are in the same locations, the size of the gradients is much less. This homogenization of the PR geography in winter (and spring) will be increased in reality by the higher amount of cloud cover in these seasons and the consequent greater importance of diffuse, as opposed to direct, radiation income.
- c) Use of the particular shading scheme employed in this study emphasizes the large areas of minimal PR receipt, appropriately shown as dark areas, on the northern flanks of Lookout Ridge and Lookout Mountain.

### The Series of Maps

When one looks at the series of maps for Dec. through June (Figs 7 through 13) one can note:

- a) There is a realistic simulated increasing amount of light on the landscape in the progress from winter to summer.
- b) There is an associated decrease of the areal extent of places of extremely low PR values as the solar radiation angles moves increasingly closer to the zenith i.e. towards the spring and summer months.
- c) Visually, there is a greater heterogeneity in PR values as one moves from winter to summer because of the larger range of PR values. Absolute maximum PR values become very large in summer but even at this time the absolute minimum PR values remain fairly low in pockets of the landscape which are topographically shaded. Calculated standard deviations provide a rather different conclusion (see below).
- d) A geographic pattern, first discussed above for the June 21 case, becomes apparent in which Lookout Creek approximately divides the Andrews Forest into an area of relatively high PR to the north of the Creek (with the exception of the north-facing slopes of the McRea Creek Valley) and relatively lower PR values to the south of the Creek. This pattern holds throughout the change of seasons.

The seasonal changes may also be investigated by examining the statistics of the 9,102 grid point values of potential radiation for each target date (Tables 1 and 2). Apart from the expected changes, three other interesting points are seen from this analysis. First, there are places which receive no direct radiation as far into the year as February. Second, the standard deviation values, which are all low because of the large sample size, show the maximum spatial variability to occur in February. This represents a trade off between on the one hand a seasonal decrease in the absolute values of direct, and direct plus diffuse radiation, and on the other hand, a trend towards more homogeneity of values as the sun reaches higher points in the sky. Third, also towards the summer months, there is a decrease in the ratio of diffuse to direct plus diffuse radiation from 0.66 at Dec 21 to 0.23 at June 21. It is expected that diffuse radiation becomes increasing more important towards the winter period but it seems that the complex topography of the Andrews exaggerates this phenomenon.

Table 1. Statistical summary of modeled values of direct radiation over the Andrews grid points. Values are in MJ/m<sup>2</sup>/day.

Date	Julian Date	Mean	Max	Min	St. Deviation
Dec 21	355	3.09	9.03	0.00	2.27
Jan 15	15	4.03	10.88	0.00	2.72
Feb 15	45	8.14	17.60	0.00	4.08
Mar 21	80	12.69	20.12	1.22	3.68
April 15	105	18.07	24.45	5.49	3.47
May 15	135	22.70	27.59	9.18	2.78
June 21	172	26.04	30.69	10.63	2.56

Table 2. Statistical summary of modeled values of direct plus diffuse radiation over the Andrews grid points. Values are in MJ/m<sup>2</sup>/day.

Date	Julian Date	Mean	Max	Min	St. Deviation
Dec 21	355	9.13	14.56	5.44	2.29
Jan 15	15	10.39	16.71	5.72	2.74
Feb 15	45	14.74	23.61	5.95	4.12
Mar 21	80	22.47	29.30	10.06	3.81
April 15	105	27.43	33.38	13.98	3.66
May 15	135	31.98	36.73	17.37	3.06
June 21	172	33.82	38.33	17.45	2.86

### Comparison of Potential Radiation Maps to Other GIS Data Layer Spatial Distributions

The spatial distributions on the PR maps may be compared spatial distributions of other biophysical factors available in the *GIS Atlas of the H. J. Andrews Forest* which is available at the Forest Science Data Bank of the Department of Forest Science, Oregon State University, and the U.S. Forest Service Pacific Northwest Research Station, Corvallis, Oregon. This atlas is an ongoing product of the H. J. Andrews LTER with new data layers being added to it as they are produced. The compilation of the Atlas dated 07/27/94 was used in this study. Interesting comparisons were noted in the case of the following data layers:

- a) As expected, there is a close general correlation between the values of PR and values of aspect. However, it should be noted that aspect values do not change through the year but PR values do. Not only do PR values have higher values towards the summer months but the values also have higher ranges between maximum and minimum values.
- b) There is a slight tendency for debris flows to be absent in the areas of relatively lower PR. This may just be a coincidence. Speculation on a physical relation might involve the fact that slopes in the transitional snow zone which receive higher values of radiant energy in the winter months are more susceptible to freeze-thaw activity than shaded slopes. Freeze-thaw activity can loosen the top layers of the soil. Shaded slopes tend to have the upper layers of the soil continually frozen for long periods of time in the winter and their top layers are not disturbed so much (Greenland, 1969, Soons and Greenland, 1970).
- c) The tree species zone distribution shows:
  - i) The Pacific Silver Fir distribution is not only at the higher elevations but also tends to be found in the rather less than maximum possible PR areas e.g. the high elevation area stretching from Frissel ridge to Carpenter Mountain has rather less PR than some of the lower elevation south-facing slopes.

ii) The same south-facing slopes tend to correspond with the transition zone between the high elevation Pacific Fir and the low elevation Western Hemlock. The extension of the transition zone south westwards towards the SW corner of the Andrews boundary also corresponds with an area of relatively high PR.

These two points also tend to apply, not unexpectedly, to the distributions shown in the potential vegetation data layer.

Recently, a set of monthly and annual precipitation maps of the Andrews have been prepared by Dr. Christopher Daly (Daly, 1995. unpublished). These maps indicate that the area of relatively low PR values identified generally south of Lookout Creek is also an area of some of the highest precipitation as well. These physical factors are consistent with the relative lack of fire frequency in this area (Swanson. pers. comm. 1995) as well as the fact that much of the old growth forest of the Andrews is also found in this location.

Further comparisons may be made with PR distributions when future data layers of the GIS Atlas become available. In addition, investigators at the Andrews are encouraged to use the PR maps listed here to search for spatial correlations between PR and phenomena on which they focus.

### Application of the Methodology to Other Areas

The methodology used in this study should be able to be applied to other areas in the Pacific Northwest and elsewhere without too much difficulty. One of the most important data sets required is a DEM of the area to be investigated. Steps for data preparation were outlined above in the sub-section of that name. One of the more difficult steps will be to find a realistic value for atmospheric transmissivity. In the absence of a nearby recording radiation station, assumptions about its value would have to be accepted. The series of appendices in this report outline in detail the steps to be taken to complete the calculations and map the resulting data. Also provided in digital form on diskette are data enabling the locations of the grid points used in this study to be identified by their UTM coordinates. These data are on a file called UTMOUT. The information on this large file may be used to add the potential radiation values of this study to the Andrews GIS. Persons using the digital information in the back of this report should read the README file first.

### DISCUSSION AND CONCLUSIONS

This study has shown that the potential direct and diffuse radiation received at the Andrews Forest is spatially and temporally highly variable. Some of the variability is expected but other parts of the variability are not obvious and are even somewhat counterintuitive. Expected results include the higher values of PR in summer than in winter and on south-facing compared to north-facing slopes and the greater relative importance of diffuse, compared to direct, radiation in the winter months. More surprising results include the identification of areas of steep PR gradients and the greater receipt of PR at the higher elevations than the lower ones. It could also be argued that Lookout Creek approximately divides the Andrews Forest into an area of relatively high PR to the north of the Creek (with the exception of the north-facing slopes of the McRea Creek Valley) and relatively lower PR values to the south of the Creek. This pattern holds throughout the change of seasons. Counter-intuitive results also include the fact that the greatest amount of spatial variability of PR occurs in late winter and early spring.

There are some interesting qualitative spatial relations between PR values and other biophysical variables in the Andrews GIS. PR values seem to be associated with the spatial distributions shown on the data layers of debris flows and predominant tree species zones. There may also be relations acting in concert with other processes and the distributions of other variables such as precipitation. Forest fire frequency is case in point.

It is in fact quite likely that PR values will have an *indirect* effect on the distributions of other biophysical variables. This is due partly to the fact that this study concentrates on potential values of PR

rather than the actual values as the PR values are mediated through the large amount of clouds which are characteristic of the climate of the location. Yet even in areas which are relatively cloud free, radiation often acts via a series of other biophysical processes and resulting spatial intercorrelations are not necessarily very strong. For example, Dubayah's (1994) study of the Rio Grande area demonstrated a certain amount of inverse correlation between  $K_{\downarrow}$  values and Normalized Difference Vegetation Index (NDVI) values from LANDSAT imagery. However, statistically, the  $K_{\downarrow}$  values only explained about 10% of the variance of the NDVI values. Dubayah correctly concludes that although  $K_{\downarrow}$  is the primary driving force for many biophysical processes, its effect is often apparent only after other intermediate processes, such as evapotranspiration, have taken place. This conclusion also applies to the Andrews Forest.

## FUTURE WORK

This study in many ways represents a beginning. Solar radiation is itself the beginning of a cascade of energy flow through the atmospheric system and the ecosystem. Future work should continue to follow the cascade to successive levels. Specifically the following steps will be of value:

- 1) The spatial analysis of the data can be continued by using geostatistical techniques. In particular, a semivariogram analysis will not only give greater information on the key spatial scales on which PR varies but also will allow a more direct comparison with the results from some other studies (e.g. Dubayah 1994).
- 2) It is important to establish the effects of clouds in attenuating the amount of potential radiation to determine finally how much radiation arrives at the surface. Even when observations are made on horizontal surfaces, large local scale variability in  $K_{\downarrow}$  in mountainous terrain is often found due to cloud amounts (Aguado, 1986, Tovar et al., 1995). Several investigators have made a start on this problem and have used approaches such as those related to the daily temperature range (Glassy and Running, 1994) and cloud observations (Munro and Young, 1982). These approaches, and others, need to be examined. Though not complete, there is a considerable set of data available for the Andrews which could be applied to this problem. These data include values recorded from a recently established sun-photometer. The application of several aspects of remote sensing technology, such as standard radiative transfer models and the daily availability of AVHRR data, hold considerable promise. The goal of this exercise would be to accurately spatially model the daily values of  $K_{\downarrow}$  over the forest.
- 3) Ecologically more important than the amount of radiation reaching the surface of the Earth is the amount actually absorbed. This depends on the albedo of the surface. It will be important to study the effect and potential effects of albedo values across the different surfaces of the forest. The consequent establishment of values of absorbed radiation will certainly be related even more closely to biophysical variables.
- 4) The establishment of  $K_{\downarrow}$  and albedo values will aid in the establishment of other variables of the radiation and surface energy balance. These variables include incoming and outgoing longwave radiation, substrate heat flow, and sensible and latent heat flow. These are the fundamental components of the physical climate and are the important linking factors to the ecosystem. Saunders and Bailey (1994) noted that "the energy budgets of sloping surfaces remain a largely untouched research problem, and nowhere is this more important than in mountainous regions".
- 5) The processes modeled in the above items must be integrated with key variables available from remote sensing technology. When this has been done, a powerful set of tools will be available to provide researchers with important bioclimatic information which can be used at a number of different scales.

The current study, although only a beginning, has provided a spatial framework into which many of the foregoing steps may be placed and in which more sophisticated modeling systems may be

established. New insights will unfold as each step is worked upon. A physical climatology will be developed to complement increasing knowledge about the synoptic and dynamic climate of the Andrews Forest. No doubt there will be many interesting and even surprising discoveries. The only certainty is that at each stage we will discover more questions.

## ACKNOWLEDGMENTS

This study has been greatly benefited by the help and encouragement of Dr. Fred Swanson. Funding was provided in part by the U.S.D.A. Forest Service, Pacific Northwest Research Station, Cooperative Agreement No. PNW 93-0477. Data sets for the H. J. Andrews Forest were provided by the Forest Science Data Bank, a partnership between the Department of Forest Science, Oregon State University, and the U.S. Forest Service Pacific Northwest Research Station, Corvallis, Oregon. Funding for these data was provided by the Long-Term Ecological Research (LTER) program and other National Science Foundation programs (NSF), Oregon State University, and U.S. Forest Service Pacific Northwest Research Station. NSF grants: DEB-7611978, BSR-9011663. The aid of Ms. Barbara Marks, Dr. Warren Cohen, and Mr. Don Henshaw is appreciated in the provision of these data sets. I am also grateful to Mr. John Moreau for help in the field. The use of Microsoft Windows and FORTRAN, ERDAS, and Golden Software Inc. SURFER software does not necessarily constitute an endorsement of those products.

## REFERENCES

- Aguado, E. 1986. Local scale variability of daily solar radiation - San Diego County, California. *Journal of Climate and Applied Meteorology*. 25:672-678.
- Blinn, T., Swanson, F.J., and McKee, A. 1988. Research Publications of the H. J. Andrews Experimental Forest, Cascade Range, Oregon, 1988 Supplement. General Technical Report. PNW-GWT-223. Portland, OR: U.S. Department of Agriculture, Forest Service, Pacific Northwest Research Station. 26 p.
- Bierlmaier, F.A., and McKee, A. 1989. Climatic summaries and documentation for the primary meteorological station, H. J. Andrews Experimental Forest, 1972-1984. USDA Forest Service, Pacific Northwest Research Station. Portland, OR. General Technical Report. PNW-GTR-223 26 pp.
- Bonan, G. B. 1988. A simulation model of environmental processes and vegetation patterns in Boreal forests: Test case Fairbanks, Alaska. Working Paper WP-88-63. International Institute for Applied Systems Analysis, Laxenberg, Austria. 63 pp.
- Bonan, G. B. 1989. A computer model of the solar radiation, soil moisture, and soil thermal regimes in Boreal forests. *Ecological Modelling*. 45:275-306.
- Budyko, M. I. 1956. *The Heat balance of the Earth's Surface*. Translated by N. I. Stepanova. U.S. Weather Bureau. Washington. D.C.
- Buffo, J., Fritschen, L., and Murphy J. 1972. *Direct solar radiation on various slopes from 0° to 60° north latitude*. USDA Forest Service. research paper. PNW-142. PNW Forest and Range Experiment Station. Portland, Oregon. 74 pp.
- Brühl, C. and Zhunkowski, W. 1983. An approximate calculation method for parallel and diffuse solar irradiances on inclined surfaces in the presence of obstructing mountains or buildings. *Archives fur Meteorologie, Geophysik, und Bioclimatologie*. Series B. 32:111-129.
- Chen, J., Franklin, J. F., and Spies, T. A. 1993. Contrasting microclimates among clearcut, edge, and interior of old-growth Douglas-fir forest. *Agricultural and Forest Meteorology*. 63:219-237.

- Dogniaux, R. (Ed.) 1994. *Prediction of Solar Radiation in Areas with a Specific Microclimate*. Kluwe Academic Publishers. Dordrecht. 107 pp.
- Dozier, J. 1980. A clear-sky spectral solar radiation model for snow-covered mountainous terrain. *Water Resources Research*. 16:709-718.
- Dozier, J. and Outcalt, S. I. 1979. An approach toward energy balance simulation over rugged terrain. *Geographical Analysis*. 11(1): 65-89.
- Duan, J., Grant, G., and Sikka, A. 1994. *Estimating incoming solar radiation at H. J. Andrews Experimental Forest*. Internal Memo. Forest Sciences Laboratory, Pacific Northwest Research Station, Corvallis, Oregon. 3 pp.
- Dubayah, R. C. 1994. Modeling a solar radiation topoclimatology for the Rio Grande River basin. *Journal of Vegetation Science*. 5:627-640.
- Dubayah, R., Dozier, J., and Davis, F. W. 1990. Topographic distribution of clear-sky radiation over the Konza Prairie, Kansas. *Water Resources Research*. 26(4)679-690.
- Duguay, C. R. 1993 Radiation modeling in mountainous terrain: Review and status. *Mountain Research and Development*. 13:339-357.
- Erbs, D. G., Klein, S. A., and Duffie, J. A. 1982. Estimation of diffuse radiation fraction, for hourly, daily, and monthly averaged global radiation. *Solar Energy*. 28:293-304.
- Ferguson, H. L., Cork, R. L., Andersen, S., and Weisman, B. 1971. *Theoretical Clear-Sky effective radiation over a small mountain basin*. Atmospheric Environment Service. Environment Canada. Climatological Studies. Number 21. 45 pp.
- Franklin, J. F., Bledsoe, C. S., and Callahan, J. T. 1990. Contributions of the Long-Term Ecological Research Program. *BioScience*. 40(7)509-523.
- Frew, J. E. 1990. *The Image Processing Workbench*. Doctoral Dissertation. Department of Geography. University of California. Santa Barbara. California.
- Fu, H. and Tajchman, S. J., and Kochenderfer, J. N. 1995. Topography and radiation exchange of a mountainous watershed. *Journal of Applied Climatology* 34:890-901.
- Fuggle, R. F. 1970. A computer program for determining direct short-wave radiation income on slopes. *Climatological Bulletin*. 7:8-16. McGill University.
- Garnier, B. J. and Ohmura, A. 1968. A method of calculating direct solar radiation on slopes. *Journal of Applied Meteorology*. 7:796-800.
- Glassy, J. M. and Running, S. W. 1994. Validating diurnal climatology logic of the MT-CLIM model across a climatic gradient in Oregon. *Ecological Applications* 4(2)248-257.
- Greenland, D. 1969. Soil heat flow investigations at Cass, South Island High Country, New Zealand. *New Zealand Journal of Agricultural Research*. 12(2)352-366.
- Greenland, D. 1994. The Pacific Northwest Context of the Climate of the H. J. Andrews Experimental Forest. *Northwest Science*. 69(2)81-96.

- Hare, F. K. and Hay, J. E. 1974. The climate of Canada and Alaska. in R. A. Bryson and F. K. Hare. (eds.) *Climates of North America*. World Survey of Climatology. Elsevier. Amsterdam. pp. 49-192.
- Hartmann, D. L. 1994. *Global Physical Climatology*. Academic Press. San Diego. 411 pp.
- Hay, J. E., 1983. Solar energy system design: the impact of mesoscale variations in solar radiation. *Atmosphere-Ocean*. 21:138.
- Holbo, H. R. and Childs, S. W. 1987. Summertime radiation balances of clearcut and shelterwood slopes in southwestern Oregon. *Forest Science*. 33(2)504-516.
- Iqbal, M. 1983. *An introduction to solar radiation*. Academic Press. New York. 390 pp.
- Isard, S. A. 1986. Evaluation of models for predicting insolation on slopes within the Colorado alpine tundra. *Solar Energy*. 36(6)559-564.
- Jensen, E. C. and Ross, C. R. 1994. *Trees to Know in Oregon*. Oregon State University Extension Circular 1450. OSU Extension Service. Corvallis. Oregon. 128 pp.
- Keith, F. and Kreider, J. F. 1978. *Principles of Solar Engineering*. Hemisphere. Washington. D.C. 778 pp.
- Klein, S A. 1977. Calculation of monthly average insolation on tilted surfaces. *Solar Energy*. 19:325-329.
- Klucher, T. M. 1979. Evaluation of models to predict insolation on tilted surfaces. *Solar Energy*. 23: 111-117.
- Kondratyev, K. Y. and Manolova, M. P. 1960. The radiation balance on slopes. *Solar Energy*. 4:14-19.
- Leavesley, G. H., Lichty, R. W., Troutman, B. M., and Saindon, L. G. 1983. Precipitation - Runoff Modeling System: User's Manual USGS Water-Resource Investigation Report 83-4238.
- Lee, Richard. 1963. *Evaluation of solar beam irradiation as a climatic parameter of mountain watersheds*. Hydrology Papers Number 2. Colorado State University. 50 pp.
- List, R. J. 1951. *Smithsonian Meteorological Tables*. 6th Rev Ed. Smithsonian Miscellaneous Collections. Vol. 114. Smithsonian Institution. Washington.
- Liu, B. Y. H. and Jordan, R. C. 1960. The interrelationship and characteristic distribution of direct, diffuse, and total solar radiation. *Solar Energy* 4:1-19.
- Liu, B. Y. H. and Jordan, R. C. 1962. Daily insolation on surfaces tilted towards the equator. *Transactions of the American Society of Heat, Refrigeration, and Air Conditioning Engineering*. 67:526-541.
- Liu, B. Y. H. and Jordan, R. C. 1963. The long-term average performance of flat-plate solar engineering collectors. *Solar Energy* 7:53-74.
- London, J. 1957. *A study of the atmospheric heat balance*. New York University. Report No AF-19(122) -165.

- McKee, A. and Bierlmaier, F. 1987. H. J. Andrews Experimental Forest, Oregon. Ch. 2. in *The climates of the Long-Term Ecological research sites*. Ed. D. Greenland. Institute of Arctic and Alpine Research. University of Colorado. Occasional Paper No 44. pp 11-17.
- McKee, A., Stonedahl, G. M., Franklin, J. F., Swanson, J. 1987. Research publications of the H. J. Andrews Experimental Forest, Cascade Range, Oregon, 1948 to 1986. General Technical Report. PNW-GWT-201. Portland, OR: U.S. Department of Agriculture, Forest Service, Pacific Northwest Research Station. 74 p.
- Munro, D. S. and Young, G. J. 1982. An operational net shortwave radiation model for glacier basins. *Water Resources Research*. 18(2)220-230.
- Nikolov, N. T. and Zeller, K. F. 1992. A solar radiation algorithm for ecosystem dynamic models. *Ecological Modelling*. 61:149-168.
- Nunez, M. 1980. The calculation of solar and net radiation in mountainous terrain. *Journal of Biogeography*. 7:173-186.
- Okanoue, M. 1957. On the intensity of radiation on any slope. (in Japanese). *Journal of the Japanese Forestry Society* 39(11):435-437.
- Oke, T. R. 1987. *Boundary Layer Climates*. Methuen. London. 2nd Ed. 435 pp.
- Saunders, I. R. and Bailey, W. G. 1994. Radiation and energy budgets of alpine tundra environments in North America. *Progress in Physical Geography*. 18(4)517-538.
- Scatterlund, D. R. and Means, J. E. 1979. *Solar radiation in the Pacific Northwest*. College of Agriculture Research Center. Washington State University. Bulletin 874. 10 pp.
- Sellers, W. D. *Physical Climatology*. University of Chicago Press. Chicago. 272 pp.
- Soons, J. M. and Greenland, D. 1970. Observations on the Growth of Needle Ice. *Water Resources Research*. 6(2)579-593.
- Star, J. L. and Estes, J. E. 1990. *Geographic Information Systems: An Introduction*. Prentice Hall. Englewood Cliffs. New Jersey. 303 pp.
- Swift, L. W. Jr. 1976. Algorithm for solar radiation on mountain slopes. *Water Resources Research* 12(1)108-112.
- Swift, L. W. Jr. and Knoerr, K. R. 1973. Estimating solar radiation on mountain slopes. *Agricultural Meteorology* 12:329-336.
- Temps, R. C. and Coulson, K. L. 1977. Solar radiation incident upon slopes of different orientations. *Solar Energy*. 19:179-184.
- Thompson, E. S., 1976. Computation of solar radiation from sky-cover. *Water Resources Research*. 12(5)859-865.
- Tovar, J., Olmo, F. J., and Alados-Arboledas, L. 1995. Local-scale variability of solar radiation in a mountainous region. *Journal of Applied Meteorology*. 34:2316-2322.
- University of Oregon Solar Radiation Laboratory. 1983. *Pacific Northwest Solar Radiation Data*. Available from the University of Oregon Library. Call Number QC911.P31 1983.

Waring, R. H., Holbo, H.R., Bueb, R. P., and Fredriksen, R. L. 1978. Documentation of meteorological data from the Coniferous Forest Biome primary station in Oregon. General Technical Report. PNW-73. Portland, OR: U.S. Department of Agriculture, Forest Service, Pacific Northwest Research Station. 23 pp.

Williams, L. D., Barry, R. D., and Andrews, J. T. 1972. Application of computed global radiation for areas of high relief. *Journal of Applied Meteorology*. 11:526-533.

Yang, X. and Miller, D. R. 1995. Calculation of potential broadband biologically active and thermal solar radiation above vegetation canopies. *Journal of Applied Meteorology*. 34:861-872.

## GLOSSARY

Albedo ( $\alpha$ ) the ratio of reflected to incoming radiation at a surface.

Azimuth angle - ( $a$ ) compass direction of the sun at any particular time.

Direct radiation ( $S$ ) is that part of the solar beam which arrives at the surface without any interaction at all with the Earth's atmosphere.

Diffuse radiation ( $D$ ) is shortwave radiation scattered downwards to the Earth's surface after striking molecules of the component atmospheric gases and aerosols together with shortwave radiation subsequently scattered back to the Earth after being reflected upwards by the Earth's surface and atmospheric components.

Global solar radiation ( $K_{\downarrow}$ ) the sum of incoming direct plus diffuse shortwave radiation.

Hour angle - the angle through which the earth must turn to bring the meridian of the observer directly under the sun.

Julian Day - the day of the year counting all the way through the year from Jan 1 = Julian Day 1 to Dec 31 = Julian day 365

Longwave radiation, also terrestrial radiation (3.0 to 100  $\mu\text{m}$ )

Net radiation ( $Q^*$ ) - the sum of incoming and outgoing flows of short and longwave radiation

Orbital vector or radius ( $d$ ) - measures the distance between the Earth and the Sun. The average distance or orbital radius is taken as 1.00. This becomes slightly higher at aphelion and slightly less at perihelion.

Optical depth ( $m$ ) is the path length through the atmosphere of the radiant beam from the sun. It is also called optical air mass number. It is the ratio of the slant path taken by the beam to the zenith distance.  $m = \sec Z_s$ .

Shortwave radiation, also solar radiation and global solar radiation: the radiation from the sun in wavelengths 0.15 to 4.0  $\mu\text{m}$ . On average 9% of shortwave radiation is UV ( $< 0.4 \mu\text{m}$ ), 49% is visible (0.4 - 0.8  $\mu\text{m}$ ), 42 % is IR ( $> 0.8 \mu\text{m}$ )

Solar constant - the average amount of shortwave radiation arriving from the sun at the outer part of the Earth's atmosphere.

Solar declination - ( $\delta$ ) the angular distance of the sun north (+ve) and south (-ve) of the equator - a function of the day of the year e.g. +23.5 = June 21 to -23.5 = Dec 22.

Zenith angle ( $Z_s$ ) - the angle between the solar beam at a given time and the line normal to a horizontal plane at the Earth's surface.

## APPENDICES

APPENDIX 1 Universal Transverse Mercator (UTM) Coordinates

APPENDIX 2 The SKIP Program

APPENDIX 3 The ELDAT Program

APPENDIX 4 The ANRAD Program and SURFER

APPENDIX 5 Data used for estimation of Extraterrestrial Radiation

### APPENDIX 1 Universal Transverse Mercator (UTM) Coordinates

Digital Elevation Model data is provided in data values at specified coordinates on a Universal Transverse Mercator (UTM) Grid. This reference system is a plane coordinate system which is based on a Transverse Mercator projection. The UTM system divides the Earth's surface into zones that are 6° longitude wide. Each zone is numbered, and the quadrilaterals of 8° latitude within a zone are lettered. Precise locations on the Earth are described in terms of north-south and east-west distances, measured in m from the origin of the appropriate UTM zone (Star and Estes, 1990).

### APPENDIX 2 The SKIP Program

Generic elevation data usually come as a Digital Elevation Model (DEM) ASCII file with information on the number of rows and columns in the file and its Universal Transverse Mercator (UTM) coordinates which give the geographic location of the data set. The grid size is also specified. If users have a large workstation machine such as a SUN then it may be possible to input these data more or less directly into ANRAD or other radiation model programs. However, for the operation of ANRAD in its present code version on microcomputers (standard of 1996), the DEM data set must be reduced to a size of about 124 x 100 data points.

The program SKIP performs this operation. It takes a 'raw' data set (in the case of this study called BASEDEM) which is in free format ASCII. The user specifies the original number of rows and columns and the "SKIP Factor" which can be between 2 and 10. If the SKIP Factor is P, the program reads every P<sup>th</sup> data point and rewrites it in a new output file called LOWRES. The user can then take LOWRES and add to the front of it the appropriate header for ANRAD data input. The number of rows and columns in LOWRES will be given by: New M = {Original M + (P+1)}/P and New N = {Original N + (P+1)}/P where M is the number of columns, N is the number of rows and P is the SKIP Factor. SKIP and all other programs in this study are written in Microsoft FORTRAN Version 5.1.

### APPENDIX 3 THE ELDAT PROGRAM

The ELDAT program takes the LOWRES data file produced by SKIP, performs 3 operations on these matrix data, and then outputs a new data file which is called ELEVDATA. The operations performed are: 1) the rows of data are reversed so as to make the DEM data compatible with ANRAD and SURFER operations, 2) a SURFER header is added at the beginning of the file, and 3) the rows of data are formatted so that they do not exceed 250 columns when viewed in a DOS, or equivalent, text editor. With respect to the last operation, if the real data in a row exceeds 250 columns the data are continued on the next lines until complete and then given an end of row record signal.

Before using the ELEVDATA file data as input for the ANRAD programs the SURFER header should be removed, the first four lines of ANRAD input information should be added, and then the file should be renamed ANDAT3.

## APPENDIX 4 The ANRAD Program and SURFER

### *Background*

The program used in this study is called ANRAD5. A digital copy of the code and an executable version is provided on a diskette at the end of this report. The program is written in MS FORTRAN version 5.1. It was originally written by Dr. Larry Williams and has been modified by the author for use on microcomputers. ANRAD5 estimates direct and diffuse radiation receipt on slopes in complex terrain. The underlying theory of the program and its application are presented in Williams et al. (1972) and in the body of this report.

The original program contained graphics routines to plot out maps of the input elevation grid and output radiation values. These routines have been removed in the version presented here. However, some of the statements in the code provided still refer back to the graphics that used to be in the program - these statements do not interfere with the operation of the program. Users wishing to add graphics capabilities compatible with their own systems will have no difficulty identifying the matrices corresponding to input and output data. SURFER software has been employed for graphical output in this application and its use is described below. ANRAD5 outputs to the C drive, data files, along with descriptive headers, which can be directly placed into the SURFER software. DIRECT is the file name for resulting computed potential direct solar radiation values. DIRDIF is the file name for potential direct plus diffuse radiation values, both relating to values in the absence of cloud cover. This version of the program can handle a 100 x 124 grid of elevational points on a PC with 4MB RAM. Larger matrices will not run on a machine of this size. However, the size of the input matrix is only limited by the machine size. The program probably could be adjusted to accept larger data matrices part by part although that would involve a major redesign of input/output and algorithm application.

### *Input Data*

Input data are of two kinds. Some data are already in the program while the majority of the data must be provided by the user. Data entered by the program are data on the fraction of extraterrestrial radiation absorbed in the atmosphere and the fraction of scattered radiation scattered downward. Default values for these are functions of latitude (Sellers, 1965. p.22). All input data should be right justified within the field in which they are entered. The program is very sensitive to input data format. If it does not operate, the user may have to alter the code paying especial attention to dimension values of arrays. It is preferable not to place these higher than necessary in order to conserve computer memory space. Elevation data lines should not exceed 250 columns when examined in the DOS or other editor.

The input data provided by the user should be provided on a file called ANDAT3 residing in the same directory as ANRAD5.EXE and are as follows:

#### **Line 1.**

The data title.  
Format (8A10) i.e. up to 80 columns/characters.

#### **Line 2.**

Set up information.

Last numbers below indicate FORTRAN format for variable. Numbers are real (floating point) unless specified as integer by I or alphanumeric (A).

LD, Latitude (Degrees) 3.0  
LM, Latitude (Minutes) 3.0

DAY, Julian day of the year 1 to 365. 4.0  
T, Transmissivity of the atmosphere (Decimal 0.00 to 1.00) 4.2  
DX, Grid spacing i.e. distance between grid points in units specified in next variable. 5.0

**Line 3.**

UX, Units of grid spacing (leave blank if in m, otherwise enter, FT, KM, or MI) 1X, A2  
M, Number of grid points in x direction. I3  
N, Number of grid points in y direction. I3  
I1, Starting column for map (The following four variables input information that will be needed if a graphics routine is added to the present program and for the program to operate properly. In this program they limit the area of the input data that is used for output and must and can be set lower than the total elevational grid if the radiation on just part of the grid needs to be examined. *They must be set at least two grid points in from the grid defined by the elevation data set.* So, for example, if the elevation data set has 128 cols. (M) and 76 rows (N) then I1, IM, J1, and JN would be respectively 3, 126, 3, and 74.) I3  
IM, Finishing column for map. I3  
J1, Starting row for map. I3  
JN, Finishing row for map. I3  
E1, Elevation of lowest contour on map. (This and the following two variables also might be needed for some mapping routines but play little part in the present version of the program) 6.0  
E2, Elevation of highest contour on map. 6.0

**Line 4.**

DE, Contour interval in units specified in next variable. [This variable is only used for some mapping programs and plays no role in the current version of ANRAD] 6.0  
UE, Units of elevation (FT or M - if left blank the program will assume m) A3  
AB, Fraction of extraterrestrial radiation absorbed in the atmosphere (If these values are not specified, default values for this *and the next variable* are used and are provided by the program from information in Sellers, 1965 *Physical Climatology* page. 22) 3.2  
FS, Fraction of scattered radiation scattered downward. 3.2

**Line 5 and successive lines.**

Elevation matrix in 50 fields per line of five digits each field.

The sample data provided with this program and report is in a file called ANDAT3. Below is an example of the first part of the file.

**Example of the first lines of ANDAT3, the data file input for the program ANRAD5.**

[Column numbers are added for convenience and should not be in the real data set which begins, in this example, at the line "DIRECT RADIATION...etc.]

```
0          1          2          3          4          5          6          7          8
1234567890123456789012345678901234567890123456789012345678901234567890

DIRECT RADIATION ANDREWS FOREST AREA DEC 21
44 12 355 68 120
  115 86 3113 3084 452 1594
000001000009000
  653 664 670 720 794 853 862 864 865 842 778 741 697 614 614 633
  841 854 875 902 921 920 920 942 968 1020 1043 1044 1047 1090 1122 1157
 1298 1283 1305 1325 1376 1433 1463 1462 1461 1462 1405 1367 1346 1341 1336 1330
```

[In this particular data set the elevation data for one row of the real data matrix are in the first three rows of the elevation part of the data file with the first two rows extending to column 250 and the third row to column 140. These three lines are repeated for further rows of the real data. Different input data sets will vary according to their original number of rows and columns. The number of lines of file elevation data per row of real elevation data is given by dividing the number of columns of real data by 25.]

### **Tabular Display**

Estimated values of radiation across the grid for the solstices and equinoxes and other target dates are provided on the accompanying diskettes and may also be obtained from the author and from the Forest Science Data Bank at the Forest Sciences Laboratory, USDA Forest Service, Pacific Northwest Research Station.

### **Graphical Display - SURFER**

Graphical display for this project was provided by the software called SURFER for WINDOWS Version 6. The output files from ANRAD5 are provided with SURFER header information already on them. The Surfer program may be used to directly make a contour plot without going through the procedure for gridding an x,y,z file. The appropriate commands are:

To make a contour plot:

- Choose Map, Contour
- Open Grid (dataflnm.grd) ok
- View - fit to window
- Choose - Change page orientation automatically - yes
- Print - fit to page

optionally add: contours, fix axis labels, change page setup from portrait to landscape.

A number of other options are available in SURFER. Some useful ones include:

#### **1) Addition of Andrews Boundary**

This is done by overlaying on the topographic map of the Andrews Forest area (Filename TOPOG1.SRF) the Andrews boundary perimeter information contained in the file PERIM1.BLN.

#### **2) Addition of location of Primet and Vanilla Leaf recording stations.**

This is done by adding to the topographic map the post map information contained in the file called CLIMSITE.DAT.

Since the ANRAD program outputs data on a grid from which the two outer data points on the original elevation grid have been removed, it is convenient to use SURFER to draw a topographic map on a scale identical to the ANRAD output maps. An elevation data matrix in a file called RADELEV may be used for this purpose. RADELEV is produced by the version of ANRAD called ANRAD4E in which the number of data columns and rows have been appropriately set. The topographic maps in this report were produced from the RADELEV data set.

APPENDX5.XLS

APPENDIX 5. Data used for Estimation of Extraterrestrial Radiation								
Computation of Extraterrestrial Radiation at the Andrews								
Computation for Solar Noon Value								
Solar constant =	1367	W/m2						
Latitude L =	44	12'	or	44.2	deg	0.771436	radians	
Hour angle (for solar noon), h =	1	=	cos h					
Computation is from equation 1 in text								
True Geocentric Distance, TGD = d/dm								
PI =	3.14159	1 deg =	0.01745329	radians	1 rad =	57.2958		
Date	Julian Day	TGD	dm/d	Solar dec deg	Solar dec rad	Sx		
						W/m2		
12/21	355	0.9834	1.01688021	-23.42	-0.40876	538.20		
1/15	15	0.9837	1.01657009	-21.2	-0.37001	960.92		
2/14	45	0.9876	1.01255569	-13.17	-0.22986	1142.05		
3/21	80	0.9961	1.00391527	3.47	0.060563	1433.33		
4/15	105	1.0032	0.99681021	9.6	0.167552	1497.19		
5/15	135	1.0108	0.98931539	18.75	0.327249	1566.77		
6/21	172	1.0162	0.98405826	23.43	0.408931	1581.58		
Computation for Daily Total								
Computation is from equation 3 in text								
Date	Julian Day	TGD	dm/d	Solar dec deg	Solar dec rad	Approx Sunrise hour angle deg	Sunrise hour angle rad	Sx
								W/m2
12/21	355	0.9834	1.01688021	-23.42	-0.40876	60	1.047198	125.77
1/15	15	0.9837	1.01657009	-21.2	-0.37001	70	1.22173	143.93
2/14	45	0.9876	1.01255569	-13.17	-0.22986	80	1.396263	207.74
3/21	80	0.9961	1.00391527	3.47	0.060563	90	1.570796	342.89
4/15	105	1.0032	0.99681021	9.6	0.167552	100	1.745329	388.71
5/15	135	1.0108	0.98931539	18.75	0.327249	110	1.919862	454.91
6/21	172	1.0162	0.98405826	23.43	0.408931	120	2.094395	484.68

APPENDX5.XLS

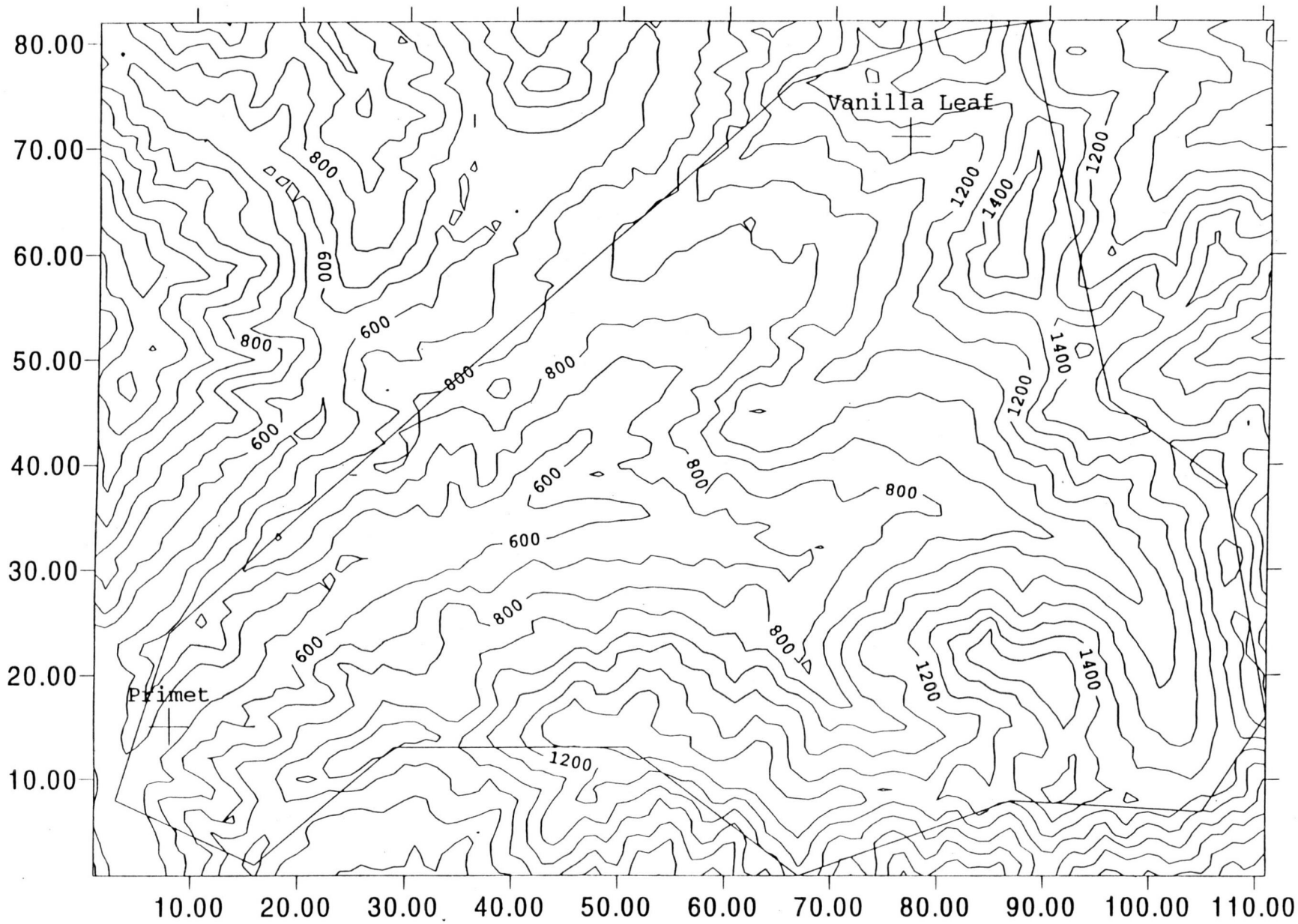
Estimation of Observed Radiation (Daily Total)										
Primet						Estimate				
Date	Julian Day	Ascending Ob	Descending Ob	Best Estimate MJ/m2	% Poss given shading	without shading	Sx MJ/m2	Trans missivity		
12/21	355		3	3	11.51	*				
1/15	15	4.9	4.4	4.6	29.69	*				
2/14	45	10	10	10	64.59	15.48	17.95	0.86		
3/21	80	16.5	16.6	16.5	82.25	20.06	29.63	0.68		
4/15	105	21	21	21	86.33	24.33	33.58	0.72		
5/15	135	25.7	25.7	25.7	88.26	29.12	39.30	0.74		
6/21	172		28.7	28.7	86.57	33.15	41.88	0.79		
		*	information unreliable at this time							
Vanmet										
Date	Julian Day	Ascending Ob	Descending Ob	Best Estimate MJ/m2	% Poss given shading of S		Sx MJ/m2	Trans missivity		
12/21	355		6.9	6.9	93.73	7.36	10.87	0.68		
1/15	15	7.8	8.8	8.3	96.76	8.58	12.44	0.69		
2/14	45	13	13.2	13.1	98.83	13.26	17.95	0.74		
3/21	80	19.7	19.5	19.6	96.79	20.25	29.63	0.68		
4/15	105	24.1	24.2	24.2	99.9	24.22	33.58	0.72		
5/15	135	28.8	28.9	28.9	99.31	29.10	39.30	0.74		
6/21	172		32.1	32.1	98.85	32.47	41.88	0.78		
Estimates from Fuggle Program										
12/21					1/15					
Potential value		Hours Not in Shade			Potential value		Hours Not in Shade			
Hour	ly	Primet	Vanmet	Hour	ly	Primet	Vanmet	Hour	ly	
5				5				5		
6				6				6		
7				7				7		
8				8				8		
9				9				9		
10			7	10			16.6	10		
11			23	11			26.7	11		
12			28.6	12			32.6	12		
13			29.4	13			33.5	13		
14			25.4	14		29.2	29.2	14		
15		16.7	16.7	15		20.2	20.2	15		
16			5.9	16		2	8.7	16		
17				17				17		
18				18				18		
19				19				19		
20				20				20		
Total Possible		Total	Total	Total Possible		Total	Total	Total		
145.1		16.7	136	173.1		51.4	167.5			
% of Possible		11.51	93.73	% of Possible		29.69	96.76			

APPENDX5.XLS

2/14				3/21			
Potential		Radiation for		Potential		Radiation for	
value		Hours Not in Shade		value		Hours Not in Shade	
Hour	ly	Primet	Vanmet	Hour	ly	Primet	Vanmet
5				5			
6				6			
7				7			
8				8			19.1
9			15	9			37.2
10			28.2	10		53.1	53.1
11			39.5	11		64.9	64.9
12		45.9	45.9	12		71.5	71.5
13		46.8	46.8	13		72.4	72.4
14		42.2	42.2	14		67.7	67.7
15		32.4	32.4	15		57.5	57.5
16		10	18.9	16		42.9	42.9
17			2.4	17			12
18				18			7.7
19				19			
20				20			
Total Possible		Total	Total	Total Possible		Total	Total
274.5		177.3	271.3	522.8		430	506
% of Possible		64.59	98.83	% of Possible		82.25	96.79
4/15				5/15			
Potential		Radiation for		Potential		Radiation for	
value		Hours Not in Shade		value		Hours Not in Shade	
Hour	ly	Primet	Vanmet	Hour	ly	Primet	Vanmet
5				5			
6				6			1
7			8.5	7			18.2
8			26.2	8		36.8	36.8
9		44.5	44.5	9		54.5	54.5
10		60.1	60.1	10		69.8	69.8
11		71.6	71.6	11		80.4	80.4
12		78.1	78.1	12		86.6	86.6
13		79	79	13		87.7	87.7
14		74.3	74.3	14		83	83
15		64.4	64.4	15		73.6	73.6
16		50.1	50.1	16		59.8	59.8
17			32.5	17		10	42.9
18			13.9	18			24.3
19			1	19			4
20				20			
Total Possible		Total	Total	Total Possible		Total	Total
604.8		522.1	604.2	727.6		642.2	722.6
% of Possible		86.33	99.90	% of Possible		88.26	99.31

APPENDX5.XLS

6/21		Radiation for	
Potential	Hours Not in Shade		
value			
Hourly	Primet	Vanmet	
5			
6		5	
7		23.3	
8	41.3	41.3	
9	58.3	58.3	
10	72.6	72.6	
11	83.1	83.1	
12	89	89	
13	89.8	89.8	
14	85.6	85.6	
15	76.6	76.6	
16	63.4	63.4	
17	15	47.1	
18		29.3	
19		6	
20			
<b>Total Possible</b>	<b>Total</b>	<b>Total</b>	
779.4	674.7	770.4	
<b>% of Possible</b>	<b>86.57</b>	<b>98.85</b>	



Axis units are 120 m (e.g 10 = 120x120 m from lower left hand corner of the map)  
North is to the top of the map. Countours are in m above msl. Straight lines  
indicate the approximate boundary of the Andrews Forest.